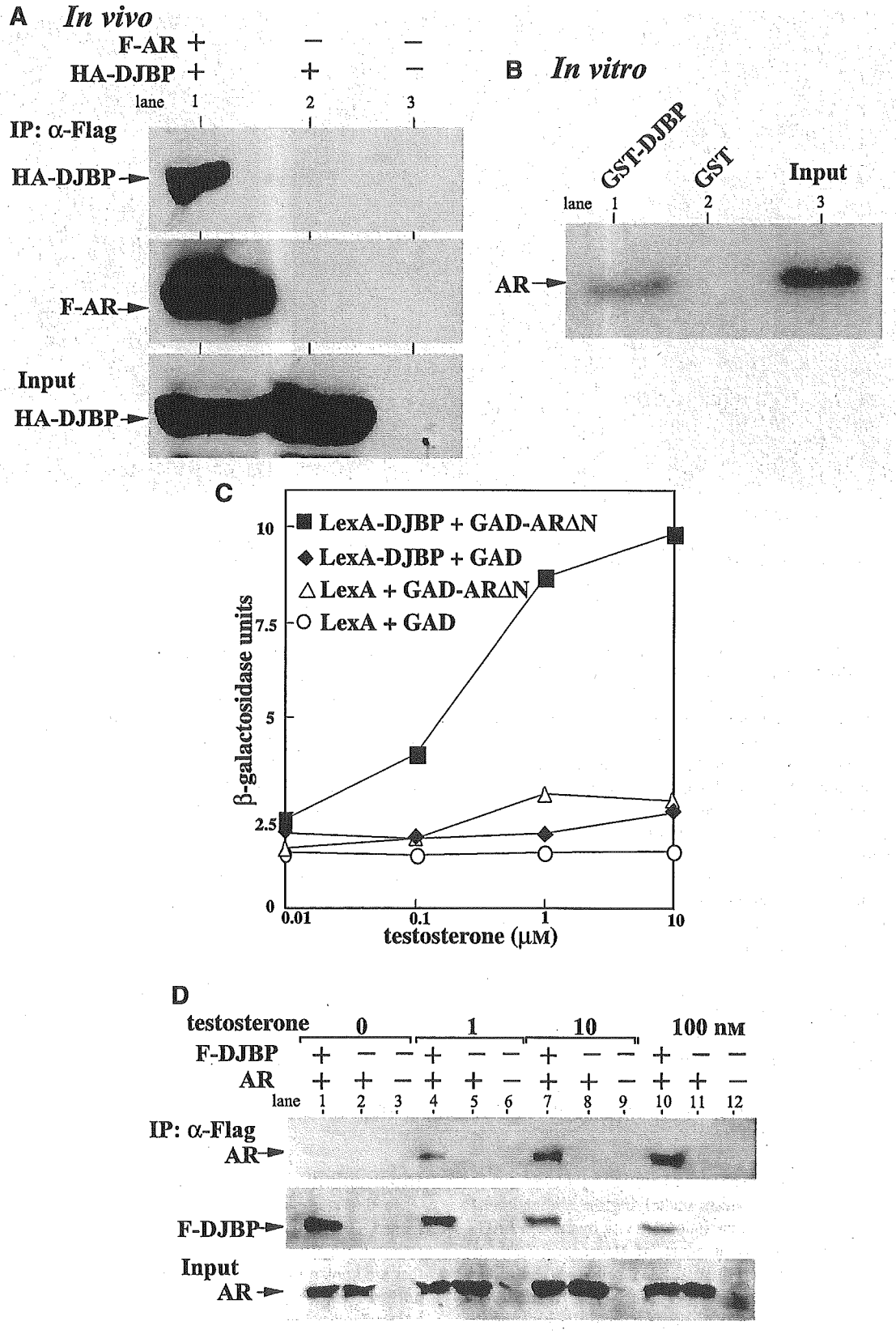
A In vivo
F-AR + — —
HA-DJBP + + —
lane 1 2 3
IP: α-Flag
HA-DJBP
F-AR
Input
HA-DJBP
B In vitro
GST-DJBP
GST
Input
lane 1 2 3
AR
C
LexA-DJBP + GAD-ARΔN
LexA-DJBP + GAD
LexA + GAD-ARΔN
LexA + GAD
β-galactosidase units
10
7.5
5
2.5
0
0.01
0.1
1
10
testosterone (μM)
D
testosterone 0 1 10 100 nM
F-DJBP + — — + — — + — — + — —
AR + + — + + — + + — + + —
lane 1 2 3 4 5 6 7 8 9 10 11 12
IP: α-Flag
AR
F-DJBP
Input
AR

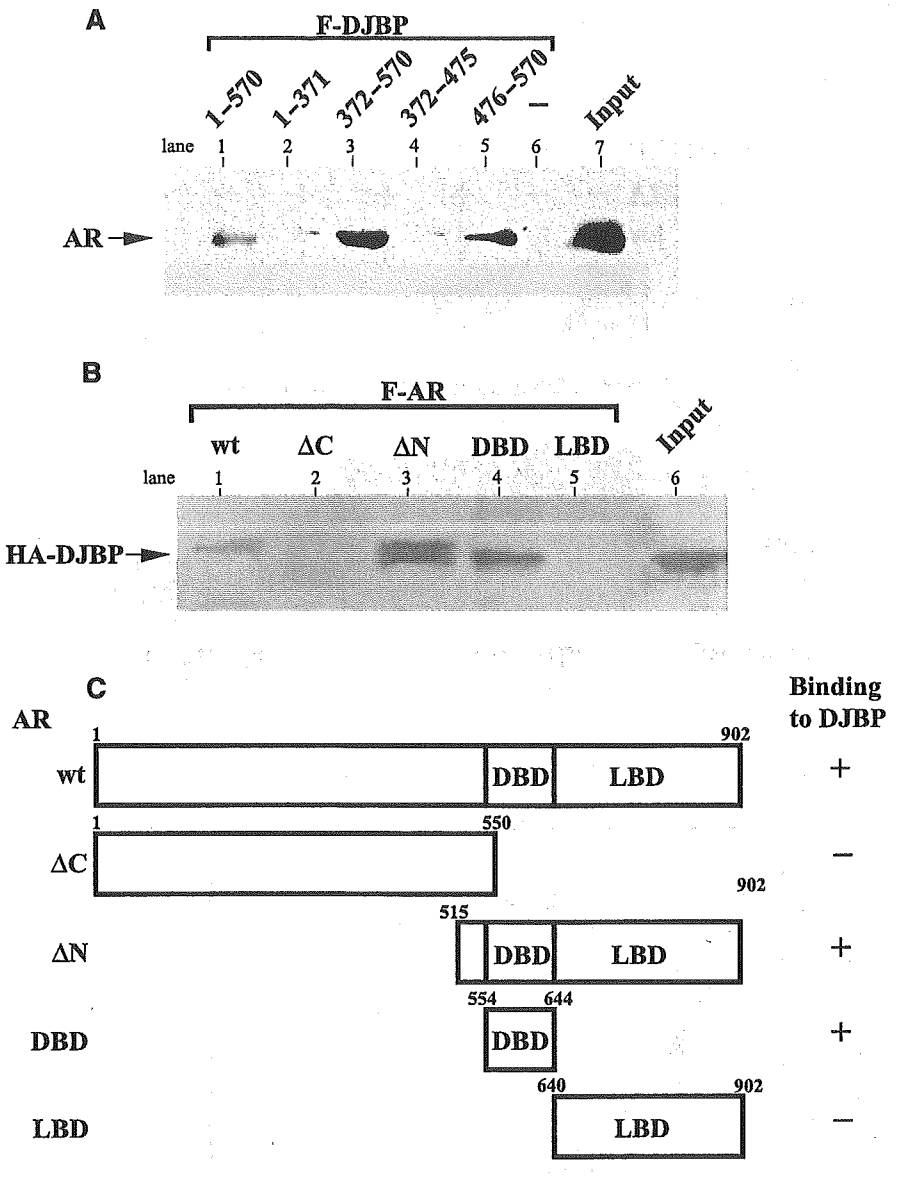

FIGURE 6. Determination of regions of binding between DJBP and AR. **A.** 293T cells cultured in the presence of 100 nM testosterone were transfected with various deletion mutants of Flag-tagged DJBP and AR. Forty-eight hours after transfection, the proteins in the cell extract were precipitated with an anti-Flag antibody and blotted with an anti-AR antibody. *Lane 7,* the cell extract used for the reactions (*Input*) was run in parallel. **B.** Cos1 cells cultured in the presence of 100 nM testosterone were transfected with various deletion mutants of Flag-tagged AR and HA-tagged DJBP. Forty-eight hours after transfection, the proteins in the cell extract were precipitated with an anti-Flag antibody and blotted with an anti-HA antibody. *Lane 6,* the cell extract used for the reactions (*Input*) was run in parallel. **C.** The AR and its deletion mutants used for the reactions are schematically shown, and the DJBP-binding activities are shown on the *right*.

and the cDNA cloned in this study appears to correspond to the 2-kb mRNA. Although the cDNA corresponding to the 7-kb mRNA is not available at present, it might be of an alternative splicing form of DJBP mRNAs.

From the results of various binding experiments *in vitro* and *in vivo*, it was found that DJBP directly binds to both DJ-1 and AR in a testosterone-dependent manner and that DJ-1 associates with AR via DJBP in a ternary complex in cells. Because AR binds to the COOH-terminal region spanning amino acids 476–570 of DJBP, in which three LXXLL-like motifs are not present, it is thought that these motifs in DJBP are not necessary for binding to the AR, like several AR-binding proteins, including BRCA1 (36), Cyclin E (37), RAF (38), TFIIH (39), CAK (39), RB (40), Ubc9 (41), c-Jun (42), and Cyclin D1 (43). DJBP, on the other hand, binds to the DNA-binding domain of the AR (AR-DBD). Because the

FIGURE 5. Interaction of DJBP with AR. **A.** 293T cells cultured in the presence of 100 nM testosterone were transfected with pcDNA3-F-AR and pcDNA3-HA-DJBP. Forty-eight hours after transfection, the proteins in cell extracts were precipitated with an anti-Flag antibody and blotted with anti-HA or -Flag antibodies. **B.** GST-DJBP and GST were expressed in *E. coli* and purified as described in "Materials and Methods." GST-DJBP or GST was mixed with ^{35}S-labeled AR synthesized *in vitro* in reticulocyte lysate and subjected to a pull-down assay. Labeled proteins bound to GST-DJBP or GST were visualized by fluorography. *Lane 4,* the AR used for the reactions (*Input*) was run in parallel. **C.** Yeast L40 cells were transformed with various combinations of LexA-DJBP, GAD-ARΔN, LexA, and GAD. The β-galactosidase activity of each colony was measured in the presence of various concentrations of testosterone. **D.** 293T cells cultured in the various amounts of testosterone were transfected with pcDNA3-AR and pcDNA3-F-DJBP. Forty-eight hours after transfection, the proteins in cell extracts were precipitated with an anti-Flag antibody and blotted with anti-AR or -Flag antibodies.

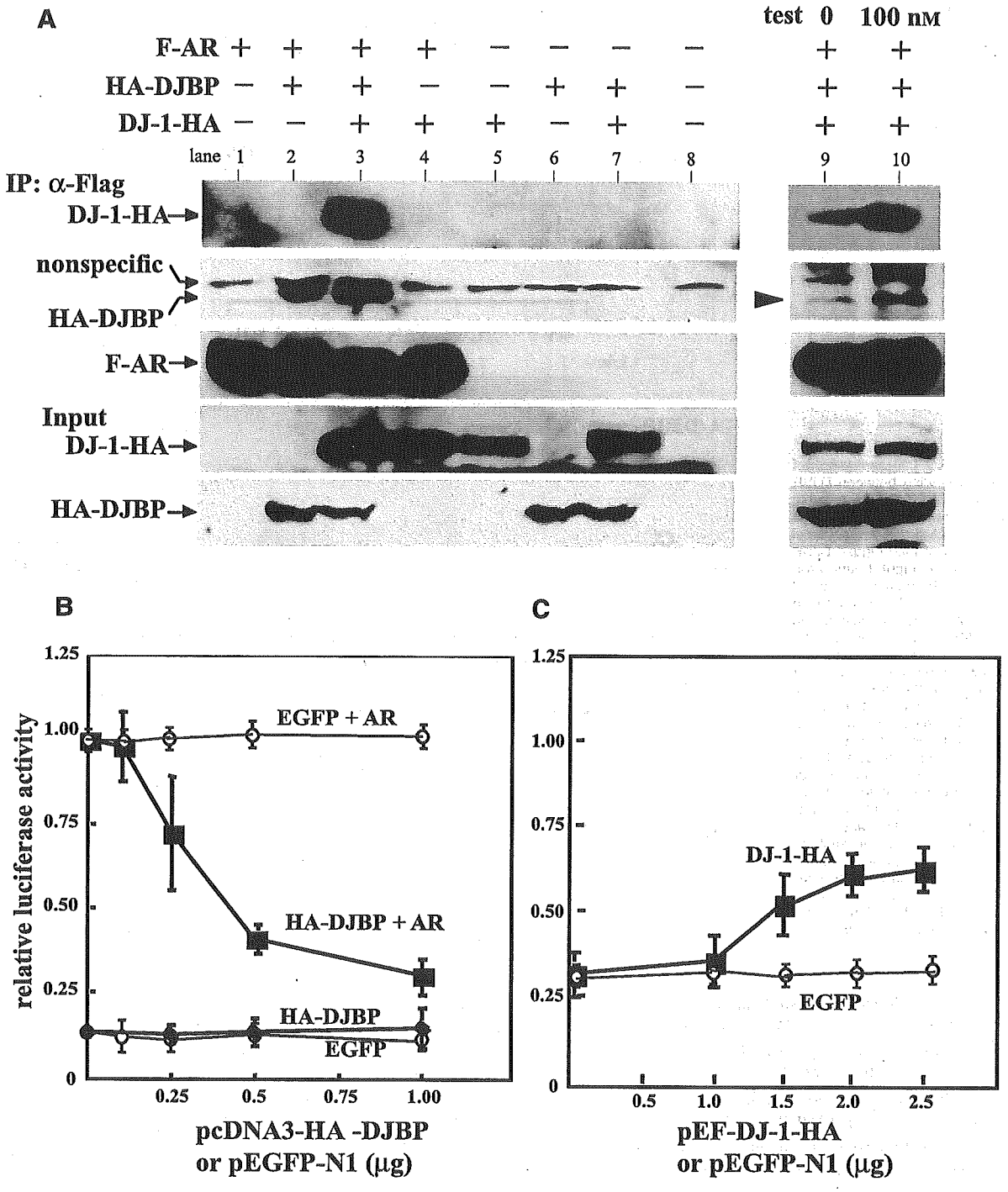

FIGURE 7. Effect of transcription activity of the AR by DJBP and DJ-1. **A.** 293T cells cultured in the presence of 100 nM testosterone were transfected with various combinations of pcDNA3-F-AR, pcDNA3-HA-DJBP, and pEF-DJ-1-HA (*lanes 1–8*). *Lanes 9 and 10,* plasmids used in lane 3 were transfected into 293T cells in the absence or presence of 100 nM testosterone. Forty-eight hours after transfection, the proteins in the cell extract were precipitated with an anti-Flag antibody and blotted with anti-Flag and anti-HA antibodies. In the lower two panels (*Input*), the cell extract used for the reactions was run in parallel and blotted with the anti-HA antibody. **B.** Cos1 cells cultured in the presence of 100 nM testosterone were transfected with 0.12 μg of pCMV-β-gal, 0.03 μg of pcDNA3-F-AR, and 1.2 μg of pARE2-TATA-Luc together with various amounts of pcDNA3-HA-DJBP or pEGFP-N1 (HA-DJBP + AR or EGFP + AR, respectively). Cos1 cells were also transfected with the same DNAs as those above except for omitting pcDNA3-F-AR (HA-DJBP or EGFP, respectively). Forty-eight hours after transfection, cell lysates were prepared and their luciferase activities were measured. **C.** Cos1 cells cultured in the presence of 100 nM testosterone were transfected with 0.12 μg of pCMV-β-gal, 0.03 μg of pcDNA3-F-AR, 1.2 μg of pARE2-TATA-Luc, and 1 μg of pcDNA3-HA-DJBP together with various amounts of pEF-DJ-1-HA or pEGFP-N1. Forty-eight hours after transfection, cell lysates were prepared and their luciferase activities were measured.

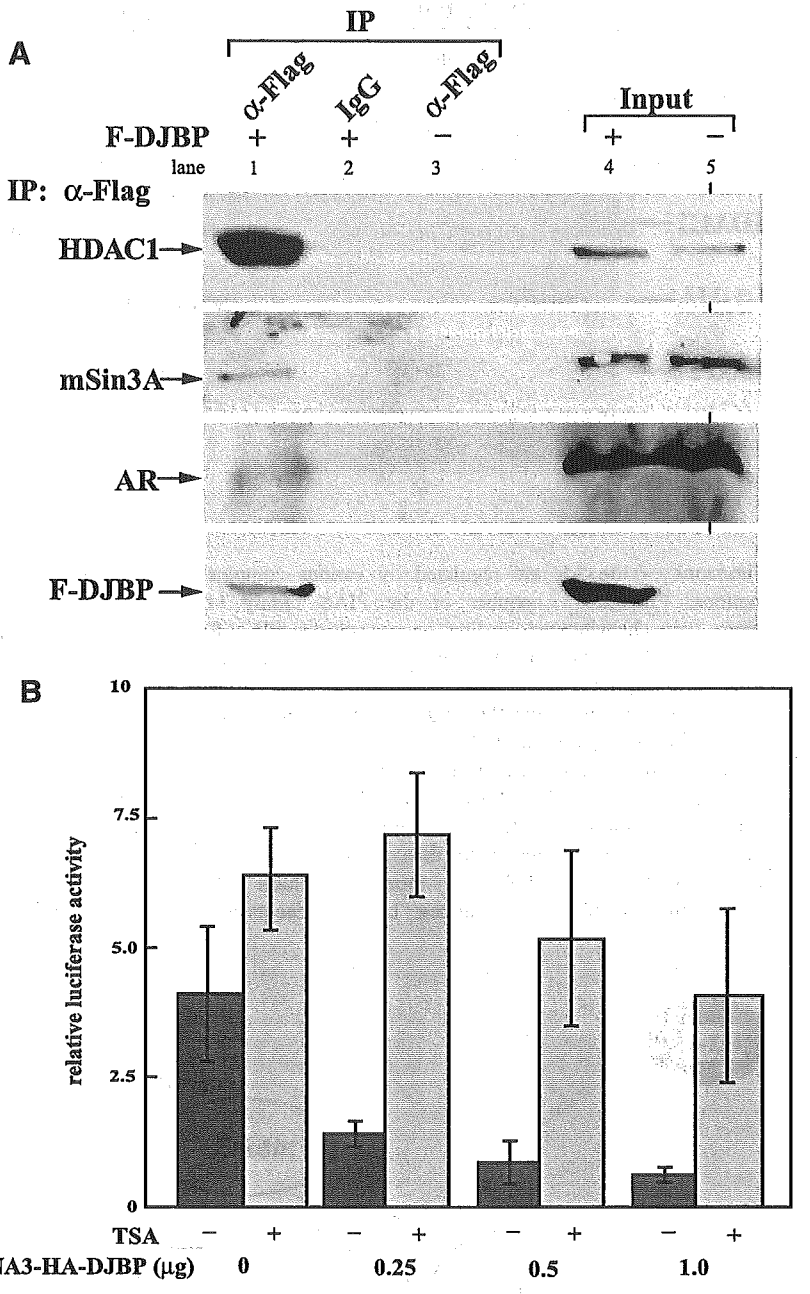

FIGURE 8. Binding of DJBP to the AR in the HDAC complex *in vivo* and effect of trichostatin A (*TSA*) on the repression activity of DJBP toward the AR. **A.** 293T cells cultured in the presence of 100 nM testosterone were transfected with an expression vector for FLAG-DJBP by the calcium phosphate precipitation technique, and the cell extract was prepared 48 h after transfection. Proteins in the extract were first precipitated with an anti-FLAG mouse monoclonal antibody or non-specific IgG, and the precipitates were immunoblotted with an anti-AR rabbit polyclonal antibody (N-20, Santa Cruz Biotechnology, Santa Cruz, CA). Proteins in the extract from non-transfected cells were similarly treated with antibodies. The same blot as that described above was reprobed with an anti-HDAC1 antibody (H-51, Santa Cruz Biotechnology) and an anti-mSin3A antibody (AK-11, Santa Cruz Biotechnology). *Lanes 4 and 5,* the proteins used for the reactions (*Input*) were run in parallel. **B.** Cos1 cells cultured in the presence of 100 nM testosterone were transfected with 0.12 μg of pCMV-β-gal, 0.03 μg of pcDNA3-F-AR, and 1.2 μg of pARE2-TATA-Luc together with various amounts of pcDNA3-HA-DJBP. Two-hundred nanomolars of TSA was added to the culture 40 h after transfection. After 48 h, cell lysates were prepared, and the luciferase activities in the lysates were measured.

amino acid sequences of DBD among nuclear receptor family proteins were well conserved, DJBP might also bind to other nuclear receptors. Of the proteins that bind to AR-DBD, SNURF (44), Ubc9 (41), and ARIP3/PIASXα (4) have been reported to associate with multiple nuclear receptors, including the AR.

DJBP was found to repress the transcription activity of AR to 30% of that without DJBP. The mechanism underlying this repression of AR activity by DJBP was assessed by the findings that DJBP recruited the corepressor complex, including HDAC1 and mSin3A. These results suggest that an active form of the AR changes into an inactive form by translocation to an inactive structure within the chromatin. Repression activity of DJBP toward the AR was sensitive to TSA, a specific inhibitor of HDAC, indicating that HDAC is involved in the transrepression pathway of the AR. The introduction of DJ-1 relieved the repressed the AR transcription activity by abrogation of DJBP-HDAC complex. It was reported that TSA augments dihydrotestosterone induction of AR levels (45). Although the results in this report suggested that the androgen-induced chromatin remodeling and transcription occur in the AR-responsive genes, the results in our study here is a first report to identify the AR-HDAC complex bridged by DJBP.

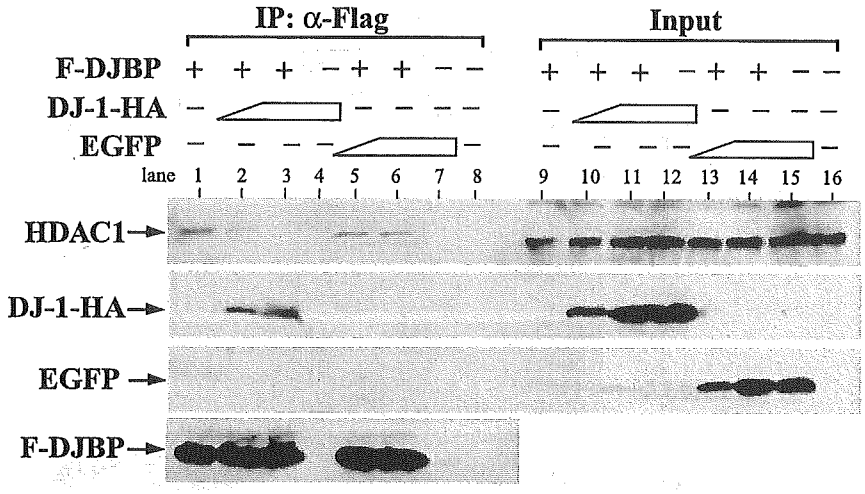

FIGURE 9. Abrogation of recruitment of HDAC complex to DJBP by DJ-1. 293T cells cultured in the presence of 100 nM testosterone were transfected with 5 μg of pcDNA3-F-DJBP, various amounts of pEF-DJ-1-HA and pEGFP-N1 by the calcium phosphate precipitation technique, and the cell extract was prepared 48 h after transfection. Proteins in the extract were first precipitated with an anti-FLAG mouse monoclonal antibody, and the precipitates were immunoblotted with an anti-HA rabbit polyclonal antibody, an anti-HDAC1 antibody, or the anti-FLAG antibody as described in Fig. 8. The 0.25-, 1-, and 1-μg pEF-DJ-1-HA or pEGFP-N1 was transfected into cells in lanes 2, 3, and 4, respectively. *Lanes 9–16,* the cell extracts used for the reactions (*Input*) were run in parallel.

Functions of the AR are regulated by various complex formations. PIASxα, a member of the PIAS family of proteins, was characterized at first as a testis-specific AR coregulator, ARIP3 (4, 5). We have shown that PIASxα inhibits the transcription activity of the AR by binding to the DNA-binding domain of the AR and that DJ-1 antagonizes this inhibition by sequestering PIASXα from the AR in CV-1, Cos1, and TM4 Sertoli cells, indicating that DJ-1 is a positive regulator of the AR (3). DJBP was found to bind to the AR, leading to formation of a ternary complex between DJ-1, DJBP, and the AR. Different to the mode of action of PIASxα on the AR, DJBP was found to inhibit AR transcription activity by recruiting histone-deacetylase complexes, including HDAC1 and mSin3, and DJ-1 was found to restore the repressed activity of the AR. These findings suggest, as schematically shown in Fig. 10, that DJ-1 restores AR activity that has been repressed by different mechanisms.

DJBP and DJ-1 were found to be expressed specifically and strongly, respectively, in the testis. Furthermore, it was found that DJ-1 was also expressed in sperm and played roles in fertilization reactions. These results suggest that DJBP also plays a role in spermatogenesis or fertilization along with DJ-1. To clarify this possibility, we are investigating the expression patterns, including location and timing, of DJBP in the testis and sperm.

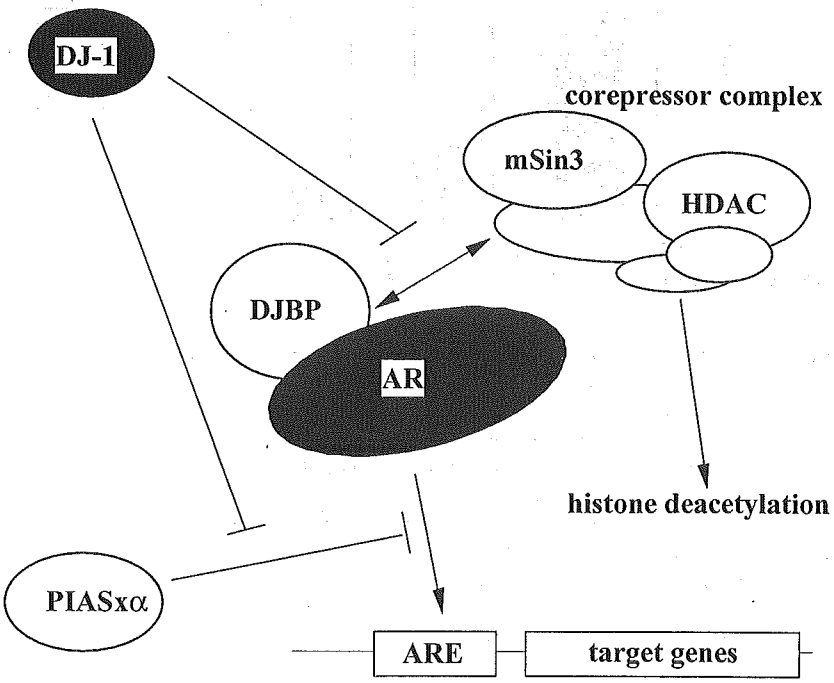

FIGURE 10. Schematic drawings of mechanisms by which DJ-1 antagonizes negative modulators of the AR by DJBP and PIASxα.

Materials and Methods

Cells

Human 293T and monkey Cos1 cells were cultured in DMEM supplemented with 10% calf serum.

Plasmids

Nucleotide sequences of the oligonucleotide used for PCR primers were as follows:

DJBP-ATG(Bam), 5′-GGATCCATGGGTCATTTT-ACAA-3′;
DJBP-ATG(Eco), 5′-GGGAATTCATGGGTCATTTT-ACAA-3′;
DJBP-193(Eco), 5′-GGGAATTCTATATAAATTGG-AAAT-3′;
DJBP-250(Eco), 5′-GGGAATTCATCACCCAGGAG-TTTG-3′;
DJBP-372(Eco), 5′-GGGAATTCGGCACTCCACCC-TTGC-3′;
DJBP-372(Bam), 5′-GGGGATCCGGCACTCCACCC-TTGC-3′;
AR-DN(Eco), 5′-GGGAATTCGGACCTTATGGG-GACA-3′;
DJBP-372(Bam), 5′-GGGGATCCGGCACTCCACCC-TTGC-3′;
DJBP-476(Bam), 5′-GGGGATCCCAGAATGCACAC-AAGA-3′;
DJBP-475(Xho), 5′-GGGAGCTCGATCTTCATCCT-GTGC-3′;
AR-DBD(Eco), 5′-GGGAATTCTACGGAGCTCTC-ACTT-3′;
AR-DBD(Xho), 5′-GGCTCGAGTACAGTCATCTT-CTGG-3′; and
AR-LBD(Eco), 5′-GGGAATTCCAGAAGATGACT-GTAT3′.

Combinations of plasmids constructed, primers, templates, and restriction enzyme sites and plasmids inserted are shown in Table 1. pGEX-F-DJ-1: The *Eco*RI-*Xho*I fragment of pGlex-DJ-1 (3) was inserted into the *Eco*RI-*Xho*I sites of pGEX-6P-1-F (46). pGAD-DJBP(1–371), pGAD-DJBP(193–371), and pGAD-DJBP(250–371): the *Eco*RI-*Sma*I fragments of pGAD-DJBP(1–570), pGAD-DJBP(93–570), and pGAD-DJBP(250–570) were inserted into the *Eco*RI-*Sma*I sites of pBluescript SK(-), and the *Eco*RI-*Xho*I fragments of these plasmids were then inserted into the *Eco*RI-*Xho*I sites of pGAD-GHX, respectively. pGLex-DJBP: The *Eco*RI-*Xho*I fragment of pGAD-DJBP(1–570) was inserted into the *Eco*RI-*Xho*I sites of pGLex (47). pcDNA3-F-DJBP(1–371): The *Eco*RI-*Xho*I fragment of pGAD-DJBP(1–371) was inserted into the *Eco*RI-*Xho*I sites of pcDNA3-F. pcDNA3-F-AR-DC: The *Eco*RI-*Hin*dIII fragment of pcDNA3-F-AR was subcloned into the *Eco*RI-*Sma*I sites of pBluescript SK(-), and the *Eco*RI-*Xho*I fragments of this plasmid were then inserted into the *Eco*RI-*Xho*I sites of pcDNA3-F. pcDNA3-F-AR-DN: The *Eco*RI-*Xho*I fragment of pGAD-AR-DN was inserted into the *Eco*RI-*Xho*I sites of pcDNA3-F.

Antibody

A fusion protein of GST and DJBP was expressed in *E. coli* MN524 and purified as described previously (3). Rabbits were immunized by the purified GST-DJBP. The anti-DJBP antibody from the rabbit serum was prepared by the affinity chromatography containing GST-DJBP, absorbed by GST, and used as the polyclonal anti-DJBP antibody.

Cloning of DJBP cDNA From a Human Testis cDNA Library by a Yeast Two-Hybrid System

Yeast L40 cells were co-transformed with expression vectors for DJ-1 fused to the LexA DNA-binding domain, pGLex-DJ-1, and human testis cDNAs from the MATCHMAKER cDNA library (Clontech Laboratories, Inc., Palo Alto, CA), which express human testis cDNAs fused to the GAL4-activating domain. Approximately 1.5×10^6 colonies were screened for expressions of HIS3 and LacZ.

Northern Blotting

A human Northern RNA blot (12 major tissues, Origene) was hybridized with ^{32}P-labeled DJBP, DJ-1, and β-actin cDNAs as probes under a highly stringent condition, and then hybridized bands were detected by autoradiography.

Table 1. Plasmid Construction

Plasmid	Template	5′-Primer	3′-Primer	Restriction Enzyme Site	Plasmid Inserted
pcDNA3-HA-DJBP	pME18S-DJBP	DJBP-ATG(Bam)	SP6	*Bam*HI, *Xho*I	pcDNA3-HA
pGEX-DJBP	pME18S-DJBP	DJBP-ATG(Bam)	SP6	*Bam*HI, *Xho*I	pGEX-6P-1
pGAD-DJBP(1–570)	pME18S-DJBP	DJBP-ATG(Eco)	SP6	*Eco*RI, *Xho*I	pGAD-GHX
pGAD-DJBP(193–570)	pME18S-DJBP	DJBP-193(Eco)	SP6	*Eco*RI, *Xho*I	pGAD-GHX
pGAD-DJBP(250–570)	pME18S-DJBP	DJBP-250(Eco)	SP6	*Eco*RI, *Xho*I	pGAD-GHX
pGAD-DJBP(372–570)	pME18S-DJBP	DJBP-372(Eco)	SP6	*Eco*RI, *Xho*I	pGAD-GHX
pGEX-DJBP(372–570)	pcDNA3-HA-DJBP	DJBP-372(Bam)	SP6	*Eco*RI, *Xho*I	pGEX-6P-1
pGAD-AR-DN	pCDNA3-F-AR	AR-DN(Eco)	SP6	*Eco*RI, *Xho*I	pGAD-GHX
pcDNA3-F-DJBP(1–570)	pcDNA3-HA-DJBP	DJBP-ATG(Bam)	SP6	*Bam*HI, *Xho*I	pcDNA3-F
pcDNA3-F-DJBP(372–570)	pcDNA3-HA-DJBP	DJBP-372(Bam)	SP6	*Bam*HI, *Xho*I	pcDNA3-F
pcDNA3-F-DJBP(476–570)	pcDNA3-HA-DJBP	DJBP-476(Bam)	SP6	*Bam*HI, *Xho*I	pcDNA3-F
pcDNA3-F-AR-DBD	pCDNA3-F-AR	AR-DBD(Eco)	AR-DBD(Xho)	*Eco*RI, *Xho*I	pcDNA3-F
pcDNA3-F-AR-LBD	pCDNA3-F-AR	AR-LBD(Eco)	SP6	*Eco*RI, *Xho*I	pcDNA3-F

Note: Combinations of plasmids constructed, primers, templates, and restriction enzyme sites and plasmids inserted are shown.

Interaction of DJBP With DJ-1 and AR in Vivo

293T cells were transfected with pcDNA3-F-DJ-1 and pcDNA3-HA-DJBP in the presence or absence of 100 nM testosterone by the calcium phosphate method (48). Forty-eight hours after transfection, the cell extract was prepared and subjected to an immunoprecipitation reaction using an anti-FLAG antibody conjugated with agarose beads (M2, Sigma Chemical Co., St. Louis, MO). The precipitates were separated on 12.5% SDS-PAGE and blotted with an anti-HA antibody (12CA5, Roche). To examine formation of a ternary complex between DJ-1, DJBP, and AR, 5 μg of pcDNA3-F-AR, 2.5 μg of pcDNA3-HA-DJBP, and 1 μg of pEF-DJ-1-HA were transfected into 293T cells in the presence of 10 mM testosterone, and then the same immunoprecipitation assay as that described above was carried out.

Interaction of DJBP with DJ-1 and AR in Vitro

F-DJ-1 and DJBP were expressed in *E. coli* as GST-fusion proteins and purified after releasing GST by digestion of GST-fusion proteins with PreScission protease (Amersham BioScience) as described previously (49). Purified F-DJ-1 and DJBP were mixed and subjected to an immunoprecipitation reaction using an anti-Flag antibody followed by an anti-DJBP antibody as described above. The anti-DJBP antibody used in this reaction was proteins of the IgG faction prepared from rabbits immunized with purified DJBP as an immunogen. To examine the binding of DJBP with the AR, purified GST-DJBP or GST was incubated with ^{35}S-AR synthesized *in vitro* using a reticulocyte lysate of a TnT-transcription-translation coupled system (Promega, Madison, WI) and subjected to a pull-down assay using an glutathione-Sepharose as described previously (49).

Immunofluorescence

Cos1 cells were transfected with 1 μg of pcDNA3-HA-DJBP or pcDNA3-F-AR by the calcium phosphate method (48). Forty-eight hours after transfection, the cells were fixed with 4% paraformaldehyde, stained with anti-DJ-1 (3), anti-AR (N-20, Santa Cruz Biotechnology), and HA antibodies, and visualized under a confocal laser microscope.

β-Galactosidase Liquid Assay

L40 cells were transformed with expression vectors for DJ-1 fused to the LexA DNA-binding domain, pGLex-DJ-1, and for various deletion mutants of DJBP fused to the GAL4-activation domain, pGAD-GHX-DJBPs. Transformed cells were cultured in YPAD medium in the presence of testosterone for 4 h, and β-galactosidase assay using cell extracts was carried out.

Luciferase Assay

Cos1 cells in 6-cm dishes were transfected with 1.3 μg of pARE2-TATA-Luc, a reporter plasmid, and 0.13 μg of pCMV-β-gal, an expression vector for β-galactosidase, by the calcium phosphate method (48). Forty-eight hours after transfection, the luciferase activity in cells was measured after normalization of the transfection efficiency with β-galactosidase activities as described previously (49).

Acknowledgments

We thank Yoko Misawa and Kiyomi Takaya for their technical assistance.

References

1. Nagakubo, D., Taira, T., Kitaura, H., Ikeda, M., Tamai, K., Iguchi-Ariga, S. M. M., and Ariga, H. *DJ-1*, a novel oncogene product which transforms mouse NIH3T3 cells in cooperation with H-*ras*. Biochem. Biophys. Res. Commun., *231:* 509–513, 1997.

2. Taira, T., Takahashi, K., Kitagawa, R., Iguchi-Ariga, S. M. M., and Ariga, H. Molecular cloning of human and mouse DJ-1 genes and identification of Sp1-dependent activation of the human DJ-1 promoter. Gene, *263:* 285–292, 2001.

3. Takahashi, K., Taira, T., Niki, T., Seino, C., Iguchi-Ariga, S. M. M., and Ariga, H. DJ-1 positively regulates the androgen receptor by impairing the binding of PIASxα to the receptor. J. Biol. Chem., *276:* 37556–37563, 2001.

4. Moilanen, A. M., Karvonen, U., Poukka, H., Yan, W., Toppari, J., Janne, O. A., and Palvimo, J. J. A testis-specific androgen receptor coregulator that belongs to a novel family of nuclear proteins. J. Biol. Chem., *274:* 3700–3704, 1999.

5. Kotaja, N., Aittomaki, S., Silvennoinen, O., Palvimo, J. J., and Janne, O. A. ARIP3 (androgen receptor-interacting protein 3) and other PIAS (protein inhibitor of activated STAT) proteins differ in their ability to modulate steroid receptor-dependent transcriptional activation. Mol. Endocrinol., *14:* 1986–2000, 2000.

6. Johnson, E. S. and Gupta, A. A. An E3-like factor that promotes SUMO conjugation to the yeast septins. Cell, *106:* 735–744, 2001.

7. Takahashi, Y., Kahyo, T., Toh-E, A., Yasuda, H., and Kikuchi, Y. Yeast Ull1/Siz1 is a novel SUMO1/Smt3 ligase for septin components and functions as an adaptor between conjugating enzyme and substrates. J. Biol. Chem., *276:* 48973–48977, 2001.

8. Jackson, P. K. A new RING for SUMO: wrestling transcriptional responses into nuclear bodies with PIAS family E3 SUMO ligases. Genes Dev., *15:* 3053–3058, 2001.

9. Kahyo, T., Nishida, T, and Yasuda, H. Involvement of PIAS1 in the sumoylation of tumor suppressor *p53*. Mol. Cell, *8:* 713–718, 2001.

10. Sachdev, S., Bruhn, L., Sieber, H., Pichler, A., Melchior, F., and Grosschedl, R. PIASy, a nuclear matrix-associated SUMO E3 ligase, represses LEF1 activity by sequestration into nuclear bodies. Genes Dev., *15:* 3088–3103, 2001.

11. Schmidt, D. and Muller, S. Members of the PIAS family act as SUMO ligases for c-Jun and p53 and repress p53 activity. Proc. Natl. Acad. Sci. USA, *99:* 2872–2877, 2002.

12. Chung, C. D., Liao, J., Liu, B., Rao, X., Jay, P. Berta, P. and Shuai, K. Specific inhibition of Stat3 signal transduction by PIAS3. Science, *278:* 1803–1805, 1997.

13. Liu, B., Liao, J., Rao, X., Kushner, S. A., Chung, C. D., Chang, D. D., and Shuai, K. Inhibition of Stat1-mediated gene activation by PIAS1. Proc. Natl. Acad. Sci. USA, *95:* 10626–10631, 1998.

14. Junicho, A., Matsuda, T., Yamamoto, T., Kishi, H., Korkmaz, K., Saatcioglu, F., Fuse, H., and Muraguchi, A. Protein inhibitor of activated STAT3 regulates androgen receptor signaling in prostate carcinoma cells. Biochem. Biophys. Res. Commun., *278:* 9–13, 2000.

15. Gross, M., Liu, B., Tan, J., French, F. S., Carey, M., and Shuai, K. Distinct effects of PIAS proteins on androgen-mediated gene activation in prostate cancer cells. Oncogene, *20:* 3880–3887, 2001.

16. Tan, J. A., Hall, S. H., Hamil, K. G., Grossman, G., Petrusz, P., and French, F. S. Protein inhibitors of activated STAT resemble scaffold attachment factors and function as interacting nuclear receptor coregulators. J. Biol. Chem., *277:* 16993–17001, 2002.

17. Kotaja, N., Vihinen, M., Palvimo, J. J., and Janne, O. A. The nuclear receptor interaction domain of GRIP1 is modulated by covalent attachment of SUMO-1. J. Biol. Chem., *277:* 30283–30288, 2002.

18. Wible, B. A., Wang, L., Kuryshev, Y. A., Basu, A., Haldar, S., and Brown, A. M. Increased K+ efflux and apoptosis induced by the potassium channel modulatory protein KChAP/PIAS3β in prostate cancer cells. J. Biol. Chem., *277:* 17852–17862, 2002.

19. Hod, Y., Pentyala, S. N., Whyard, T. C., and El-Maghrabi, M. R. Identification and characterization of a novel protein that regulates RNA-protein interaction. J. Cell. Biochem., *72:* 435–444, 1999.

20. Le Naour, F., Misek, D. E., Krause, M. C., Deneux, L., Giordano, T. J., Scholl, S., and Hanash, S. M. Proteomics-based identification of RS/DJ-1 as a novel circulating tumor antigen in breast cancer. Clin. Cancer Res., *7:* 3328–3335, 2001.

21. Mitsumoto, A., Nakagawa, Y., Takeuchi, A., Okawa,, K., Iwamatsu, A., and Takanezawa, Y. Oxidized forms of peroxiredoxins and DJ-1 on two-dimensional gels increased in response to sublethal levels of paraquat. Free Radic. Res., *35:* 301–310, 2001.

22. Mitsumoto, A. and Nakagawa, Y. DJ-1 is an indicator for endogenous reactive oxygen species elicited by endotoxin. Free Radic. Res., *35:* 885–893, 2001.

23. Klinefelter, G. R., Laskey, J. W., Ferrell, J., Suarez, J. D., and Roberts, N. L. Discriminant analysis indicates a single sperm protein (SP22) is predictive of fertility following exposure to epididymal toxicants. J. Androl., *18:* 139–150, 1997.

24. Wagenfeld, A., Yeung, C. H., Strupat, K., and Cooper, T. G. Shedding of a rat epididymal sperm protein associated with infertility induced by ornidazole and α-chlorohydrin. Biol. Reprod., *58:* 1257–1265, 1998.

25. Wagenfeld, A., Gromoll, J., and Cooper, T. G. Molecular cloning and expression of rat contraception associated protein 1 (CAP1), a protein putatively involved in fertilization. Biochem. Biophys. Res. Commun., *251:* 545–549, 1998.

26. Welch, J. E., Barbee, R. R., Roberts, N. L., Suarez, J. D., and Klinefelter, G. R. SP22: a novel fertility protein from a highly conserved gene family. J. Androl., *19:* 85–93, 1998.

27. Wagenfeld, A., Yeung, C. H., Shivaji, S., Sundareswaran, V. R., Ariga, H., and Cooper, T. G. Expression and cellular localization of contraception-associated protein 1. J. Androl. *21:* 954–963, 2000.

28. Whyard, T. C., Cheung, W., Sheynkin, Y., Waltzer, W. C., and Hod, Y. Identification of RS as a flagellar and head sperm protein. Mol. Reprod. Dev., *55:* 189–196, 2000.

29. Klinefelter, G. R., Welch, J. E., Perreault, S. D., Moore, H. D., Zucker, R. M., Suarez, J. D., Roberts, N. L., Bobseine, K., and Jeffay, S. Localization of the sperm protein SP22 and inhibition of fertility *in vivo* and *in vitro*. J. Androl., *23:* 48–63, 2002.

30. Okada, M., Matsumoto, K., Niki, T., Taira, T., Iguchi-Ariga, S. M. M., and Ariga, H. DJ-1, a target protein for an endocrine disrupter, participates in the fertilization in mice. Biol. Pharm. Bull., *25:* 853–856, 2002.

31. Quigley, C. A., De Bellis, A., Marschke, K. B., el-Awady, M. K., Wilson, E. M., and French, F. S. Androgen receptor defects: historical, clinical, and molecular perspectives. Endocr. Rev., *16:* 271–321, 1995.

32. Brown, T. R. Human androgen insensitivity syndrome. J. Androl., *16:* 299–303, 1995.

33. McPhaul, M. J., Marcelli, M., Zoppi, S., Griffin, J. E., and Wilson, J. D. Genetic basis of endocrine disease. 4. The spectrum of mutations in the androgen receptor gene that causes androgen resistance. J. Clin. Endocrinol. & Metab., *76:* 17–23, 1993.

34. Yong, E. L., Ghadessy, F., Wang, Q., Mifsud, A., and Ng, S. C. Androgen receptor transactivation domain and control of spermatogenesis. Rev. Reprod., *3:* 141–144, 1998.

35. Janne, O. A., Moilanen, A. M., Poukka, H., Rouleau, N., Karvonen, U., Kotaja, N., Hakli, M., and Palvimo, J. J. Androgen-receptor-interacting nuclear proteins. Biochem. Soc. Trans., *28:* 401–405, 2000.

36. Rebbeck, T. R., Kantoff, P. W., Krithivas, K., Neuhausen, S., Blackwood, M. A., Godwin, A. K., Daly, M. B., Narod, S. A., Garber, J. E., Lynch, H. T., Weber, B. L., and Brown, M. Modification of BRCA1-associated breast cancer risk by the polymorphic androgen-receptor CAG repeat. Am. J. Hum. Genet., *64:* 1371–1377, 1999.

37. Yamamoto, A., Hashimoto, Y., Kohri, K., Ogata, E., Kato, S., Ikeda, K., and Nakanishi, M. Cyclin E as a coactivator of the androgen receptor. J. Cell Biol., *150:* 873–880, 2000.

38. Migliaccio, A., Castoria, G., Di Domenico, M., de Falco, A., Bilancio, A., Lombardi, M., Barone, M. V., Ametrano, D., Zannini, M. S., Abbondanza, C., and Auricchio, F. Steroid-induced androgen receptor-oestradiol receptor β-Src complex triggers prostate cancer cell proliferation. EMBO J., *19:* 5406–5417, 2000.

39. Lee, D. K., Duan, H. O., and Chang, C. From androgen receptor to the general transcription factor TFIIH. Identification of cdk activating kinase (CAK) as an androgen receptor NH(2)-terminal associated coactivator. J. Biol. Chem., *275:* 9308–9313, 2000.

40. Yeh, S., Miyamoto, H., Nishimura, K., Kang, H., Ludlow, J., Hsiao, P., Wang, C., Su, C., and Chang, C. Retinoblastoma, a tumor suppressor, is a coactivator for the androgen receptor in human prostate cancer DU145 cells. Biochem. Biophys. Res. Commun., *248:* 361–367, 1998.

41. Poukka, H., Aarnisalo, P., Karvonen, U., Palvimo, J. J., and Janne, O. A. Ubc9 interacts with the androgen receptor and activates receptor-dependent transcription. J. Biol. Chem., *274:* 19441–19446, 1999.

42. Bubulya, A., Wise, S. C., Shen, X. Q., Burmeister, L. A., and Shemshedini, L. c-Jun can mediate androgen receptor-induced transactivation. J. Biol. Chem., *271:* 24583–24589, 1996.

43. Knudsen, K. E., Cavenee, W. K., and Arden, K. C. D-type cyclins complex with the androgen receptor and inhibit its transcriptional transactivation ability. Cancer Res., *59:* 2297–2301, 1999.

44. Moilanen, A. M., Poukka, H., Karvonen, U., Hakli, M., Janne, O. A., and Palvimo, J. J. Identification of a novel RING finger protein as a coregulator in steroid receptor-mediated gene transcription. Mol. Cell. Biol., *18:* 5128–5139, 1998.

45. List, H. J., Smith, C. L., Rodriguez, O., Danielsen, M., and Riegel, A. T. Inhibition of histone deacetylation augments dihydrotestosterone induction of androgen receptor levels: an explanation for trichostatin A effects on androgen-induced chromatin remodeling and transcription of the mouse mammary tumor virus promoter. Exp. Cell Res., *252:* 471–478, 1999.

46. Koike, N., Maita, H., Taira, T., Ariga, H., and Iguchi-Ariga, S. M. M. Identification of heterochromatin protein 1 (HP1) as a phosphorylation target by Pim-1 kinase and the effect of phosphorylation on the transcriptional repression function of HP1. FEBS Lett., *467:* 17–21, 2000.

47. Ono, T., Kitaura, H., Ugai, H., Murata, T., Yokoyama, K. K., Iguchi-Ariga, S. M. M., and Ariga, H. TOK-1, a novel p21Cip1-binding protein that cooperatively enhances p21-dependent inhibitory activity toward CDK2 kinase. J. Biol. Chem., *275:* 31145–31154, 2000.

48. Graham, F. J. and Van der Eb, A. J. A new technique for the assay of infectivity of human adenovirus 5 DNA. Virology, *52:* 456–467, 1973.

49. Niki, T., Izumi, S., Saëgusa, Y., Taira, T., Takai, T., Iguchi-Ariga, S. M. M., and Ariga, H. MSSP promotes the ras/myc cooperative cell transforming activity by binding to C-MYC. Genes Cells, *5:* 127–140, 2000.

MOLECULAR REPRODUCTION AND DEVELOPMENT 66:391–397 (2003)

Immunocytochemical Localization of DJ-1 in Human Male Reproductive Tissue

KAORU YOSHIDA,[1,2] YOKO SATO,[1,2] MIKI YOSHIIKE,[1,2] SHIARI NOZAWA,[1,2] HIROYOSHI ARIGA,[1,3] AND TERUAKI IWAMOTO[1,2]*

[1]*Core Research for Evolutional Science and Technology, Japan Science and Technology Corporation, Kawaguchi, Saitama, Japan*
[2]*Department of Urology, St. Marianna University School of Medicine, Sugao, Miyamae-ku, Kawasaki, Japan*
[3]*Graduate School of Pharmaceutical Sciences, Hokkaido University, Kita-ku, Sapporo, Japan*

ABSTRACT DJ-1 was identified as an activated *ras*-dependent oncogene product, and was also found to be an infertility-related protein (contraception-associated protein 1; CAP 1) that was reduced in rat spermatozoa treated with ornidazole, one of the endocrine disrupting substances that causes reversible infertility in rats. CAP 1 is present in spermatozoa but is not detectable in the epididymal fluid of fertile rats and appears to be shed from sperm during treatment with ornidazole. To determine the functions of DJ-1 in the human reproductive system as a target protein of endocrine active substances, we identified the localization of DJ-1 in human testis, epididymis, ejaculated spermatozoa, and seminal plasma. DJ-1 was present in cells existing in the seminiferous tubules and Leydig cells. Some strong expressions were observed in Leydig cells and Sertoli cells, suggesting a relation with spermatogenesis via androgen receptor (AR). In ejaculated spermatozoa, DJ-1 existed on the surface of the posterior part of head and the anterior part of the midpiece. DJ-1 was also present on sperm flagella when the antibody penetrated the plasma membrane, suggesting that there are two putative roles in fertilization, one is binding to the egg, and the other is flagella movement. In contrast to previous findings, we detected DJ-1 in seminal plasma of fertile men. These results demonstrate that DJ-1 in human seminal plasma is not only from spermatozoa but also from the testis and epididymis. It is suggested that DJ-1 may play an important and as yet uncharacterized role in spermatogenesis and fertilization in humans. *Mol. Reprod. Dev. 66: 391–397, 2003.*

Key Words: fertilization; spermatozoa; testis; 2D electrophoresis

INTRODUCTION

DJ-1 was identified as a novel candidate for the oncogene product that transformed mouse NIH3T3 cells in cooperation with activated *ras* (Nagakubo et al., 1997). The human *DJ-1* gene is mapped at chromosome 1p36.2-p36.3, where a hot spot of chromosome abnormalities has been reported in several tumors (Taira et al., 2001). Northern blots indicated expression of DJ-1 in many human tissues, with the highest level exhibited in the testis. DJ-1 is translocated from the cytoplasm to nuclei during the cell cycle after mitogen stimulation, suggesting that DJ-1 has a growth-related function (Nagakubo et al., 1997). However, the mechanism by which cells are transformed has not been clarified.

The RS protein in rat hepatoma cells as the regulatory subunit of an RNA binding protein (RBP) was identified and found to be identical to DJ-1 (Hod et al., 1999). Recently the other group reported that the autoantibodies of RS/DJ-1 present in sera from patients with breast cancer (Le Naour et al., 2001). Furthermore, contraception-associated protein 1 (CAP 1) or SP22, a rat homologue of human DJ-1, was identified as a key protein related to the infertility of male rats exposed to sperm toxicants such as ornidazole and epichlorohydrin in which DJ-1 in the sperm and epididymis decreased in parallel with the following infertility (Klinefelter et al., 1997; Wagenfeld et al., 1998a,b; Welch et al., 1998). It was shown that DJ-1/CAP 1/SP22 is the first protein clearly related to male infertility (Klinefelter et al., 1997; Wagenfeld et al., 1998b; Welch et al., 1998). Sperm from ornidazole-treated rats showed no significant differences in the percentage of motile spermatozoa compared with those from vehicle-treated males (Oberlander et al., 1994), but there was a decrease in velocities depending on the substance provided (Yeung et al., 1995). Motile sperm from ornidazole-fed males failed to fertilize ova in vitro (Bone et al., 2000), suggesting that factors other than motility may be involved in the resulting infertility. The SP22 protein was found in extracts of cauda epididymal sperm and their amounts were correlated with the ability of sperm to

Grant sponsor: Grants-in-aid from the Ministry of Education, Science, Culture and Sport of Japan.

*Correspondence to: Teruaki Iwamoto, Department of Urology, St. Marianna University School of Medicine, 2-16-1, Sugao, Miyamae-ku, Kawasaki 216-8511, Japan. E-mail: t4iwa@marianna-u.ac.jp

Received 31 January 2003; Accepted 3 March 2003
Published online in Wiley InterScience (www.interscience.wiley.com).
DOI 10.1002/mrd.10360

fertilize eggs in vivo (Klinefelter et al., 1997; Okada et al., 2002). In a subsequent study, Klinefelter et al. (2002) generated the specific anti-SP22 antibodies and showed these antibodies were capable of inhibiting the fertility of cauda epididymal rat sperm using both in utero insemination and in vitro insemination. Moreover, these antibodies inhibited in vitro fertilization of both zona-intact and zona-free hamster oocytes, suggesting that SP22 played a role in both the zona penetration and membrane fusion steps of fertilization (Klinefelter et al., 2002). Two-dimensional (2D) gel electrophoresis of the proteins in cauda and corpus epididymidal fluid from infertile rats demonstrated the appearance of CAP 1, a protein originating and shed from sperm as a result of drug treatment (Wagenfeld et al., 1998b). In addition to its expression in spermatocytes and spermatids, DJ-1 is also expressed in the sperm head and is translocated to the cytoplasmic side of sperm after the toxicant treated rats, suggesting that DJ-1 plays a role in fertilization (Welch et al., 1998; Wagenfeld et al., 2000; Whyard et al., 2000).

Takahashi et al. (2001) recently identified PIASxα as a DJ-1 binding protein in culture cell lines. The protein inhibitor of activated STATxα (signal transducers and activators of transcription) (PIASxα) inhibited the androgen receptor (AR) minimal promoter activity in monkey CV1 cells, and DJ-1 antagonized the repression activity of PIASxα to AR by absorbing PIASxα from the AR–PIASxα complex (Takahashi et al., 2001). These results suggest that DJ-1 is a positive regulator of the AR. However, the localization of DJ-1 is not clear in human testis. Moreover, there is no evidence about the localization of DJ-1/CAP 1/SP22 in rat testis Sertoli cells and Leydig cells in which the AR may localize. The exact roles of DJ-1 in spermatogenesis and fertilization have not been determined particularly in humans. To obtain more information on the cellular localization of DJ-1 in human reproductive tissue and spermatozoa, we performed immunodetection on human male reproductive tissue, ejaculated spermatozoa, and extracts from these samples.

MATERIALS AND METHODS

Sample Preparations

Semen samples were collected from human male volunteers by masturbation in a sterile container after at least 48 hr of abstinence. Each semen sample was liquefied for 15–30 min at 37°C before sample preparations. For sperm preparations, semen samples were obtained from healthy young volunteers with unknown fertility (n = 4, 20–24 years of age). The semen was layered on 5 ml of 85% Percoll (Sigma, St. Louis, MO) and a continuous Percoll density gradient made with mixing the semen and the Percoll solution. All the Percoll solutions were buffered with HEPES-buffered saline (10 mM HEPES, pH 8.0, 130 mM NaCl, 4 mM KCl, 1 mM $CaCl_2$, 0.5 mM $MgCl_2$, and 14 mM fructose). Following centrifugation (1,300*g*) for 30 min at 20°C, the spermatozoa accumulating at the bottom of the tube was collected. For seminal plasma preparations, semen samples were collected from male partners of fertile couples (n = 30, 25–42 years of age) and liquefacted semen was centrifuged to eliminate the solid materials. The supernatants as seminal plasma were placed in aliquots and frozen at −80°C until analysis.

Tissue specimens of the testis were obtained from eight men, 25–75 years of age (Table 1). We selected the specimens that showed higher means of Johnsen score counts (JS) (Johnsen, 1970) than 5.0. In these specimens, we found the seminiferous tubule where JS value was higher than 8.0. The epididymis was from a 28-year-old patient, undergoing orchiectomy for a testicular tumor. Tissues were fixed with 10% formaline in PBS for 12 hr at 25°C and embedded in paraffin. The 5–7 μm thick sections were cut with a microtome and mounted on MAS coated glass slides (Mitsubishi Biochemical Laboratory, Tokyo). These sections were provided for immunohistochemistry after deparaffinization and dehydration.

The anti DJ-1 monoclonal antibody was purchased from manufacturer (3E8, Medical and Biological Laboratories, Ina., Japan). This antibody was prepared against GST-human DJ-1 fusion protein corresponding to full length amino acids (1–187 a.a.) and detects human DJ-1 on Western blot with total cell lysate from human cell line. No cross reactivity was observed to mouse cell line. Before the following experiments, we confirmed that the antibody has no reactivity to mouse and rat testis (data not shown).

The Ethical Committee/Institutional Review Board of St. Marianna University approved the study. Informed consent was obtained from volunteers before the use of their tissue or semen for research.

Electrophoresis and Western Blotting

Isoelectric focusing was carried out in an immobilized pH gradient (IPG) gel strip on the IPGphor isoelectric focusing apparatus (Amersham Biosciences, Tokyo) to reach a total of 25 kVh for a pH 4–7 IPG strip (7 cm). Samples were solubilized with lysis buffer containing 8 M urea, 2% 3-[(3-cholamidopropyl)-dimethylammonio]-1-propanesulfonate) (CHAPS), 18 mM dithiothreitol (DTT) for 15 min at room temperature. Protein

TABLE 1. Testis Specimens for Immunohistochemistry

Specimens	Operation	Mean JS
Testicular tumor (n = 5)	Orchiectomy	
1		6.00
2		7.44
3		7.75
4		7.62
5		2.63[a]
Prostate cancer (n = 1)	Orchiectomy	5.10
Oligozoospermia (n = 1)	Biopsy	
L		7.20
R		6.28
Valicocele (n = 1)	Biopsy	
L		6.08
R (valicocele)		5.49

[a]In this case, there are a few seminiferous that show high JS.

concentration was measured by the bicinchroninic acid assay (Smith et al., 1985) using BSA as a standard. Each 10 μg sample per one strip was applied to rehydration buffer containing 8 M urea, 2% CHAPS, 18 mM DTT, and 0.5% IPG buffer (pH 4–7) during reswelling of the IPG strip. The first equilibration solution for SDS gel electrophoresis contained 30% (w/v) glycerol, 6 M urea, 1% (w/v) DTT, and 2% SDS (w/v) in 50 mM Tris-HCl pH 8.8. The second portion of equilibration solution contains 2.5% (w/v) iodoacetamide instead of DTT. Both equilibration steps usually lasted 15 min at room temperature.

Molecular weight separations were carried out on 10–20% (w/v) polyacrylamide gradient SDS gels. These gels were silver stained or electroblotted onto polyvinylidene difluoride (PVDF) membranes and the membranes were blocked for 1 hr at 37°C with a solution of 5% (w/v) nonfat dried milk in Tris-buffered saline (20 mM pH 7.8) supplemented with Tween 20 (0.05%; TBS-T). The membranes were incubated with the anti-DJ-1 monoclonal antibody (3E8, MBL) at 1 μg/ml in TBS-T containing 5% (w/v) nonfat dried milk for 30 min at 37°C. The control incubations were performed by the antibody preabsorbed with excess recombinant human DJ-1 protein expressed in and purified from *E. coil*. After three washes in TBS-T for 5 min, the membranes were incubated with goat anti-mouse IgG conjugated with alkaline phosphatase (BioRad, Hercules, CA) at a dilution of 1:3,000 in TBS-T for 30 min at 37°C. Following several washes in TBS-T, the detection was performed with 5-bromo-4-chloro-3-indolylphosphate/nitro blue tetrazolium (BCIP/NBT) (Sigma).

Immunohistochemistry and Immunocytochemistry

The tissue sections were blocked for endogenous peroxidase activity with 3% hydrogen peroxide in methanol for 15 min. Nonspecific antibody binding was blocked in PBS containing 10% normal goat serum for 1 hr at room temperature. The sections were incubated with the anti-DJ-1 monoclonal antibody (3E8, MBL) at 5 μg/ml in PBS containing 10% normal goat serum for 1 hr at 37°C. The control incubations were performed by the antibody preabsorbed with excess recombinant human DJ-1 protein. Each section was treated with peroxidase-conjugated anti-mouse IgG (Histofine Simple Stain MAX PO; Nichirei, Tokyo) for 30 min at room temperature and developed with 3-amino-*n*-ethylcarbazole (Nichirei) for visualization. Sections were counterstained with Mayer hematoxylin for 10 sec and mounted in aqueous permanent mounting solution (Nichirei).

An aliquot of Percoll washed spermatozoa suspended in PBS was spotted on glass slides, air-dried, and fixed with 4% paraformaldehyde (PFA) for 5 min at room temperature or with methanol at −20°C for 10 min. These preparations were blocked in PBS containing 1% BSA for 30 min at 37°C and incubated with the anti-DJ-1 monoclonal antibody (3E8, MBL) at 6 μg/ml or normal mouse IgG as a negative control at 6 μg/ml in PBS containing 1% BSA for 1 hr at 37°C. Following washing, these preparations were treated with fluorescein isothiocyanate (FITC)-conjugated anti-mouse antibody (Vector Laboratories, Burlingame, CA) at 5 μg/ml for 30 min at 37°C. These preparations were mounted in the solution containing 90% (v/v) glycerol and 1,4-diazabicyclo [2,2,2] octane (DABCO) and visualized using epifluorescent microscope.

RESULTS

Western Blot Analysis of DJ-1 in Testis, Seminal Plasma, and Spermatozoa

Western blot analysis of proteins from human testis, seminal plasma, and spermatozoa showed one clear band for anti-DJ-1 monoclonal antibody positive at M_r 24×10^{-3} (Fig. 1B). In spermatozoa, most DJ-1 was extracted with demembranation solution (0.1% Triton X-100, 0.2 M sucrose, 0.025 M potassium glutamate, 0.035 M Tris-HCl pH 8.0, and 1 mM DTT) at the first extraction. Then the signal was decreased in the second extraction with lysis buffer containing 8 M urea, 2% CHAPS. From 2D Western blots of human testis, seminal plasma, and spermatozoa, major four spots of DJ-1 positive (isoelectric points [pIs] = 5.7, 5.8, 6.1, 6.4, or 6.7) were observed in each specimen (Fig. 2). The pIs and molecular weights of these spots were identical except pI 6.7 spot in seminal plasma (Fig. 2E). The pI 6.7 spot in seminal plasma was not separated in this gel because it was located close to the end of the strip, however, in the pH3-10 IPG strip, it moved to approximately pI 6.7 (data not shown). The volumes of these DJ-1 positive spots depended on its origin and specimen used. Inclusion of excess of recombinant human DJ-1 protein during the immunoreaction abolished the detection of DJ-1 (data not shown).

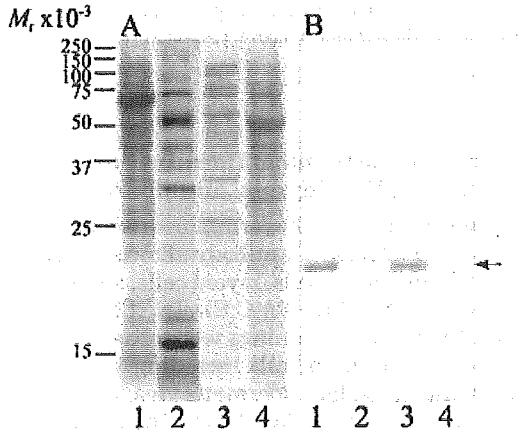

Fig. 1. Western blot analysis of DJ-1 with SDS–PAGE gel electrophoresis. Protein samples prepared from testis (**lane 1**), seminal plasma (**lane 2**), and ejaculated spermatozoa (**lanes 3, 4**). The same membrane was stained with CBBR (**A**). Anti DJ-1 positive band is at M_r 24×10^{-3} in each lane (**B**, allow). Spermatozoa extracted first with 0.1% Triton 100-X (lane 3) and secondly with 8 M urea, 2% 3-[(3-cholamidopropyl)-dimethylammonio]-1-propanesulfonate) (CHAPS) (lane 4). The positions of the molecular weight markers are indicated in the left.

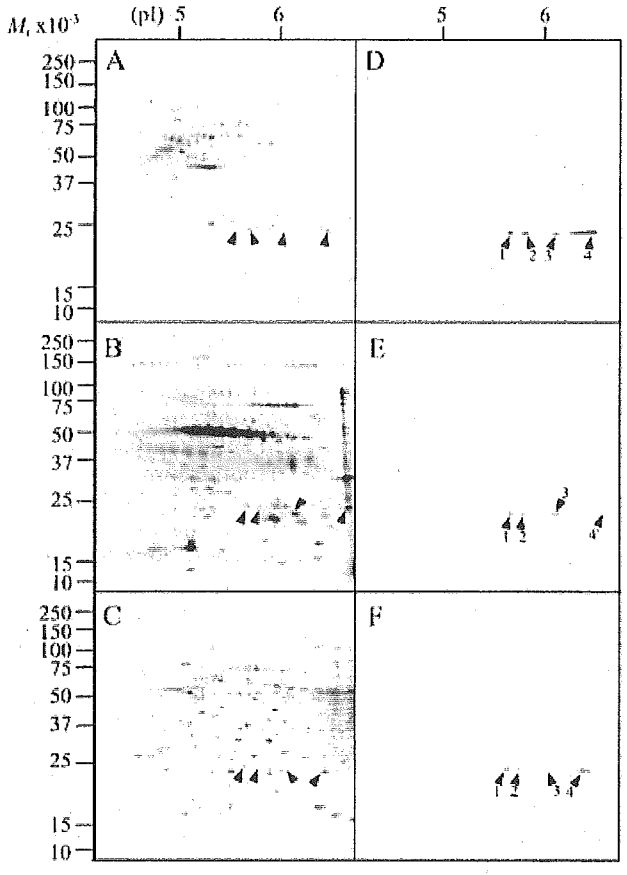

Fig. 2. Western blot analysis of DJ-1 with 2D gel electrophoresis. The silver stained profile of proteins were in the **left column** and immunoblot with anti DJ-1 monoclonal antibody were in the **right column**. Protein samples prepared from testis (**A, D**), seminal plasma (**B, E**), and ejaculated spermatozoa (**C, F**). Allow heads indicate DJ-1 positive spots (1 for pI 5.7, 2 for pI 5.8, 3 for pI 6.1, 4 for pI 6.4, or 4′ for pI 6.7). The positions of the molecular weight markers and the pI markers are indicated in the left and on above, respectively.

Immunocytochemical Localization of DJ-1 in Testis, Epididymis, and Spermatozoa

Immunostaining of 10% formaline fixed human testis sections with anti-DJ-1 antibody showed intense positive signals in Sertoli cells, myoid cells, spermatogonia, and Leydig cells (Fig. 3A,C,E). In the seminiferous tubules, the positive stainings were observed in Sertoli cells and also in germ cells including spermatogonia, primary and secondary spermatocytes, and round and elongated spermatids (Fig. 3C,D). In Leydig cells, we observed the most intense signals of DJ-1 (Fig. 3A,E). DJ-1 was localized in both the cytoplasm and nucleus in Leydig cells (Fig. 3E). We confirmed this staining pattern by the use of anti DJ-1 polyclonal antibody that was prepared by Nagakubo et al. (1997) and was used in rat testis by Wagenfeld et al. (2000) (data not shown). Control incubations with anti DJ-1 monoclonal antibody preabsobed by excess recombinant human DJ-1 protein showed no immunological staining (Fig. 3B,G). Some late elongating spermatids also showed staining, however, some of them were not stained (Fig. 3C). The intense staining was also observed in epididymis (Fig. 3F). DJ-1 was localized in epithelial cells of the epididymis and spermatozoa in the lumen (Fig. 3F).

Immunolocalization of DJ-1 in Ejaculated Spermatozoa

Figure 4 shows indirect immunofluorescence localization of DJ-1 in human ejaculated spermatozoa. DJ-1 is abundant in the methanol fixed human sperm tail and the posterior part of the head and the anterior part of the midpiece (Fig. 4C). In the 4% PFA fixed sperm, DJ-1 appeared on the surface of the posterior part of the head and the anterior part of midpiece and there is weak staining in the tail (Fig. 4A). A ring-like structure in the head suspected to be the equatorial segment was also stained in both the 4% PFA fixed and methanol fixed sperm. However, in the control incubations, some fluorescence was observed in the equatorial zone of methanol fixed sperm head (Fig. 4D).

DISCUSSION

In the present study, a detailed localization pattern of DJ-1 in human male reproductive system at the protein levels is described. Western blot analyzes in our study showed that the DJ-1 existed in extracts from testis, spermatozoa, and seminal plasma at M_r 24×10^{-3}. This molecular weight was different from the M_r 28×10^{-3} of rat CAP 1/SP22 as previously reported and also from the M_r 20×10^{-3} of human DJ-1 as predicted, however, the difference depended on the method of sample preparation and on running gel. In the isoforms of DJ-1 that we found, the most alkalitic one was DJ-1/pI 6.4 in spermatozoa and testis, or DJ-1/pI 6.7 in seminal plasma. It is suggested that DJ-1/pI 6.4 is an unmodified form of DJ-1 because the predicted pI of human DJ-1 is 6.4. As an indicator of oxidative stress status, DJ-1 was identified in human endothelial cell lines with two isoforms; DJ-1/pI 6.2 decreased and DJ-1/pI 5.8 increased in response to sublethal levels of paraquat (Mitsumoto et al., 2001). The DJ-1/pI 6.1 isoform we found in testis, spermatozoa, and seminal plasma may correspond to the DJ-1/pI 6.2 and DJ-1/pI 5.8 in the human endothelial cell lines, respectively. Four different isoforms of DJ-1 were found in each extract but each spot volume depended on the sample, and also the total volumes of DJ-1 were different among each specimen. The modification mechanism of DJ-1 is not yet known; these isoforms may reflect the status of the human male reproductive system. Moreover, when spermatozoa were exposed to oxidative stress after ejaculation (Sikka et al., 1995), DJ-1 on the surface of spermatozoa may act as a scavenger of reactive oxygen species.

DJ-1 was first identified as a novel oncogene product that transforms mouse NIH3T3 cells in collaboration with activated *ras* (Nagakubo et al., 1997) and was later found to be a homologous protein, CAP 1/SP22, related to male rat infertility caused by exposure of rats to

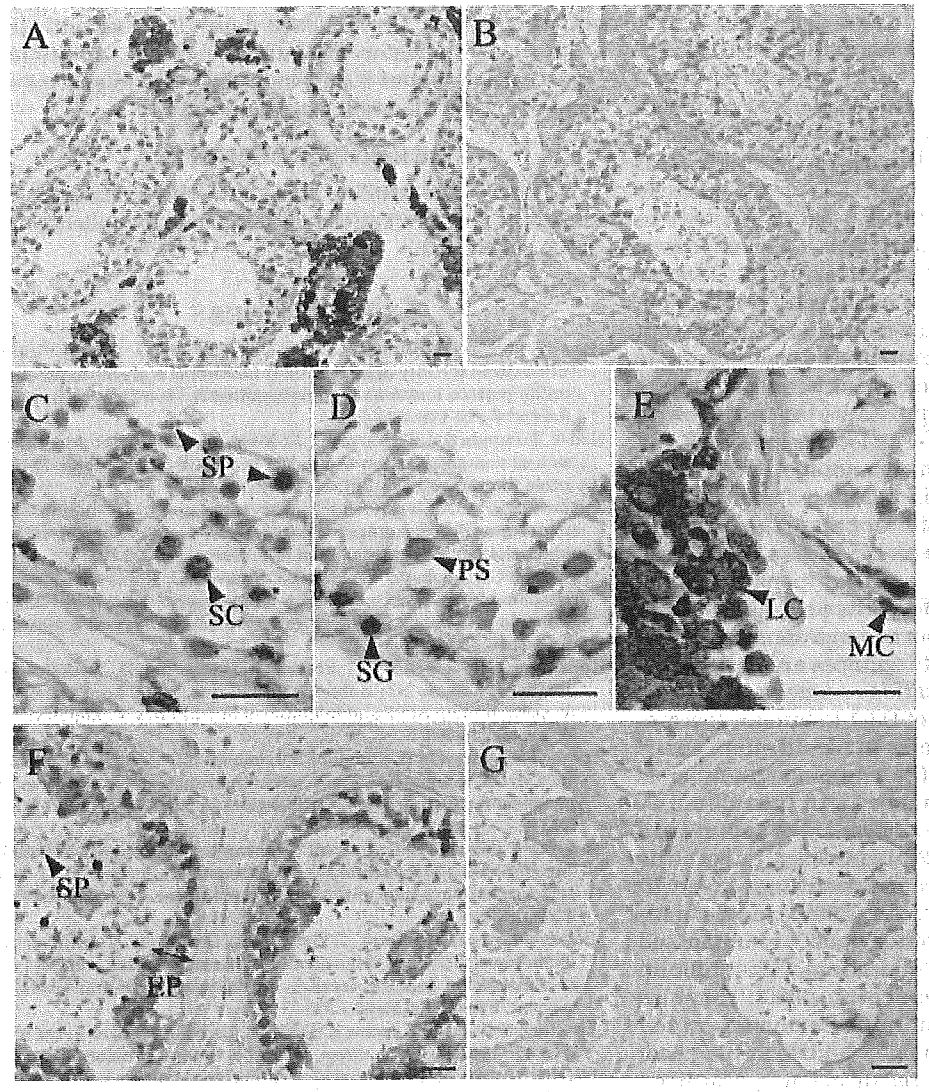

Fig. 3.

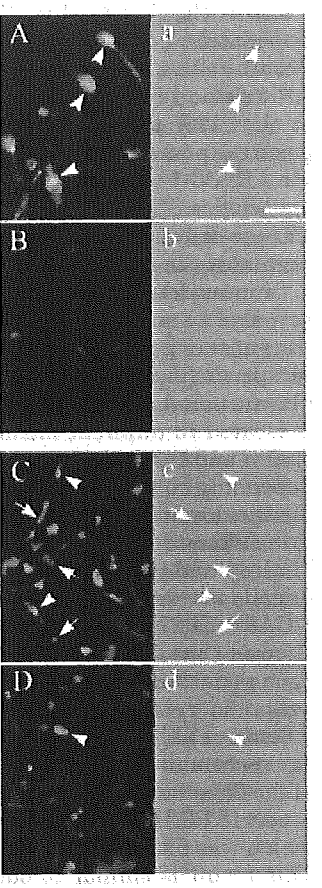

Fig. 4.

Fig. 3. Localization of DJ-1 in testis and epididymis by immunohistochemical staining. Negative control incubations were performed with anti DJ-1 antibody preabsorbed by excess recombinant human DJ-1 protein (**B, G**). Intense signals were in Sertoli cells (**C**, SC) and spermatogonia (**D**, SG) in the seminiferous tubule, and also in Leydig cells (**E**, LC), DJ-1 localized both in nucleus and in cytoplasm. Myoid cells were also stained (E, MC). Elongated spermatids, round spermatids (C, SP) and primary spermatocytes (D, PS) were slightly stained. In the epidydimis, intense signals were in epithelium cells (**F**, EP) and spermatozoa in the efferent ductules (F, SP). Scale bars = 20 μm.

Fig. 4. Immunofluorescence localization of DJ-1 in ejaculated spermatozoa. Fluorescein isothiocyanate (FITC) fluorescence represent in 4% paraformaldehyde (PFA) fixed sperm (**A, B**) and methanol fixed sperm (**C, D**). Negative control in that anti DJ-1 antibody is replaced with nonspecific mouse IgG (B, D). Capital letters, fluorescent microscopic images obtained using FITC-labeled secondary anti-mouse IgG; small letters, phase contrast microscopic images. DJ-1 localized in the posterior part of head and the anterior part of midpiece (A, C, allow heads), and in the tail (C, allows). The around equatorial segment of the head was immunoreactive with nonspecific mouse immunoglobulin (D, allow head). Scale bar = 10 μm.

the male reproductive toxicants such as ornidazole or epichlorohydrin (Klinefelter et al., 1997; Wagenfeld et al., 1998b). DJ-1 is thus suggested to have at least two functions: a function in somatic cells and a function in germ cells. With regard to the function in somatic cells, Takahashi et al. (2001) recently showed that DJ-1 acts as a positive regulator of AR by preventing PIASxα from binding to AR in human cell lines. In rat germ cells, the mRNA of CAP 1/SP22 is expressed in stages from pachytene spermatocytes and finally is expressed in

the anterior–ventral region of the sperm head, which was suggested thought to be essential for fertilization (Wagenfeld et al., 2000). Recently, Klinefelter et al. (2002) generated highly specific polyclonal and monoclonal antibodies to SP22 and showed that SP22 localized from round spermatids to elongated spermatids in rat testis. Contrary to these findings about rat testis, our result is the first to show that DJ-1 exists not only in spermatids, but also in spermatogonia, spermatocytes, Sertoli cells, and Leydig cells in human testis. Because AR exists in Sertoli cells and Leydig cells (Van Roijen et al., 1995), the DJ-1 in these cells, shown here, suggests the possible role as a regulator of spermatogenesis via AR. DJ-1 was also localized in epithelial cells of the epididymis (Fig. 3F) and the prostate (data not shown). These results support that DJ-1 co-localizes with AR and regulates the gene expression depending AR.

Immunodetection of DJ-1 in ejaculated spermatozoa revealed a staining of the posterior part of the head and the anterior part of the midpiece. DJ-1 was also detected in sperm flagella when the antibody penetrated the plasma membrane. These differences suggest that DJ-1 is located in different membrane environments of the sperm and the exposures of its epitopes are changeable depending on the different fixation regimens. These two distinct localization patterns of DJ-1 in human spermatozoa showed two putative roles in fertilization; one is binding and penetrating to the egg, and the other is flagella movement. Recent studies about the role of DJ-1/CAP 1/SP22 existing on the surface of the sperm head showed that DJ-1/CAP 1/SP22 is involved in both the zona penetration and membrane fusion steps of fertilization in rats (Klinefelter et al., 2002) and in mice (Okada et al., 2002). On the other hand, in human and rat spermatozoa, RS/DJ-1 is co-localized with β-tubulin of the flagellar axoneme (Whyard et al., 2000). They also reported RS/DJ-1 is abundant in the human sperm tail which was fixed with methanol, with little in the head. This result is similar to our result about sperm fixed with methanol, and supports that RS/DJ-1 may play some role in flagellar motility.

In contrast to previous findings (Wagenfeld et al., 2000), we detected DJ-1 in seminal plasma of fertile men. Human semen, even if from fertile men, contains every type of abnormal spermatozoa in morphology in contrast to semen from other species (Kruger et al., 1986). The present results showed that DJ-1 is abundant in testis and also in epididymis. These findings imply that the DJ-1 in seminal plasma is not only from spermatozoa but also from the testes and epididymis. The initial observations suggesting the involvement of DJ-1 with fertility came from the appearance of the protein in epididymal fluid of ornidazole-fed male rats and a decline of the protein from sperm extracts using silver stained 2D gels (Wagenfeld et al., 1998b). However, in humans, DJ-1 was already present in seminal plasma of fertile men as reported in this article. Moreover, our preliminary findings from recent studies suggests that the DJ-1 levels in seminal plasma are decreased in men presenting with infertility compared with fertile men (unpublished data). To deal with the DJ-1 as an indicator for human fertility, additional investigations about its physiological role in spermatogenesis and fertilization are required.

ACKNOWLEDGMENTS

We thank the stuff of male infertility clinic at St. Marianna University School of Medicine for collection of tissue specimens.

REFERENCES

Bone W, Jones NG, Kamp G, Yeung CH, Cooper TG. 2000. Effect of ornidazole on fertility of male rats: Inhibition of a glycolysis-related motility pattern and zona binding required for fertilization in vitro. J Reprod Fertil 118:127–135.

Hod Y, Pentyala SN, Whyard TC, El-Maghrabi MR. 1999. Identification and characterization of a novel protein that regulates RNA–protein interaction. J Cell Biochem 72:435–444.

Johnsen SG. 1970. Testicular biopsy score count—A method for registration of spermatogenesis in human testes: Normal values and results in 335 hypogonadal males. Hormones 1:2–25.

Klinefelter GR, Laskey JW, Ferrell J, Suarez JD, Roberts NL. 1997. Discriminant analysis indicates a single sperm protein (SP22) is predictive of fertility following exposure to epididymal toxicants. J Androl 18:139–150.

Klinefelter GR, Welch JE, Perreault SD, Moore HD, Zucker RM, Suarez JD, Roberts NL, Bobseine K, Jeffay S. 2002. Localization of the sperm protein SP22 and inhibiton of fertility in vivo and in vitro. J Androl 23:48–63.

Kruger TF, Menkveld R, Stander FS, Lombard CJ, Van der Merwe JP, van Zyl JA, Smith K. 1986. Sperm morphologic features as a prognostic factor in in vitro fertilization. Fertil & Steril 46:1118–1123.

Le Naour F, Misek DE, Krause MC, Deneux L, Giordano TJ, Scholl S, Hanash SM. 2001. Proteomics-based identification of RS/DJ-1 as a novel circulating tumor antigen in breast cancer. Clin Cancer Res 7:3328–3335.

Mitsumoto A, Nakagawa Y, Takeuchi A, Okawa K, Iwamatsu A, Takanezawa Y. 2001. Oxidized forms of peroxiredoxins and DJ-1 on two-dimensional gels increased in response to sublethal levels of paraquat. Free Radic Res 35:301–310.

Nagakubo D, Taira T, Kitaura H, Ikeda M, Tamai K, Iguchi-Ariga SM, Ariga H. 1997. DJ-1, a novel oncogene which transforms mouse NIH3T3 cells in cooperation with ras. Biochem Biophys Res Commun 231:509–513.

Oberlander G, Yeung CH, Cooper TG. 1994. Induction of reversible infertility in male rats by oral ornidazole and its effects on sperm motility and epididymal secretions. J Reprod Fertil 100:551–559.

Okada M, Matsumoto K, Niki T, Taira T, Iguchi-Ariga SM, Ariga H. 2002. DJ-1, a target protein for an endocrine disrupter, participates in the fertilization in mice. Biol Pharm Bull 25:853–856.

Sikka SC, Rajasekaran M, Hellstrom WJ. 1995. Role of oxidative stress and antioxidants in male infertility. J Androl 16:464–481.

Smith P, Krohn R, Hermanson G, Mallia A, Gartnert F, Provenzano M, Fujimoto E, Goeke N, Olson B, Klenk D. 1985. Measurement of protein using bicinchoninic acid. Anal Biochem 150:76–85.

Taira T, Takahashi K, Kitagawa R, Iguchi-Ariga SM, Ariga H. 2001. Molecular cloning of human and mouse *DJ-1* genes and identification of Sp1-dependent activation of the human DJ-1 promoter. Gene 263:285–292.

Takahashi K, Taira T, Niki T, Seino C, Iguchi-Ariga SM, Ariga H. 2001. DJ-1 positively regulates the androgen receptor by impairing the binding of PIASx alpha to the receptor. J Biol Chem 276:37556–37563.

Van Roijen JH, Van Assen S, Van Der Kwast TH, De Rooij DG, Boersma WJ, Vreeburg JT, Weber RF. 1995. Androgen receptor immunoexpression in the testes of subfertile men. J Androl 16:510–516.

Wagenfeld A, Gromoll J, Cooper TG. 1998a. Molecular cloning and expression of rat contraception associated protein 1 (CAP1), a protein

putatively involved in fertilization. Biochem Biophys Res Commun 251:545–549.

Wagenfeld A, Yeung CH, Strupat K, Cooper TG. 1998b. Shedding of a rat epididymal sperm protein associated with infertility induced by ornidazole and alpha-chlorohydrin. Biol Reprod 58:1257–1265.

Wagenfeld A, Yeung CH, Shivaji S, Sundareswaran VR, Ariga H, Cooper TG. 2000. Expression and cellular localization of contraception-associated protein. J Androl 21:954–963.

Welch JE, Barbee RR, Roberts NL, Suarez JD, Klinefelter GR. 1998. SP22: A novel fertility protein from a highly conserved gene family. J Androl 19:385–393.

Whyard TC, Cheung W, Sheynkin Y, Waltzer WC, Hod Y. 2000. Identification of RS as a flagellar and head sperm protein. Mol Reprod Dev 55:189–196.

Yeung CH, Oberlander G, Cooper TG. 1995. Effects of the male antifertility agent ornidazole on sperm function in vitro and in the female genital tract. J Reprod Fertil 103:257–264.

THE JOURNAL OF BIOLOGICAL CHEMISTRY
Vol. 278, No. 33, Issue of August 15, pp. 31380–31384, 2003
Printed in U.S.A.

The Crystal Structure of DJ-1, a Protein Related to Male Fertility and Parkinson's Disease*

Received for publication, June 4, 2003
Published, JBC Papers in Press, June 8, 2003, DOI 10.1074/jbc.M305878200

Kazuya Honbou‡, Nobuo N. Suzuki‡§, Masataka Horiuchi‡§, Takeshi Niki§¶, Takahiro Taira§¶, Hiroyoshi Ariga§¶, and Fuyuhiko Inagaki‡§‖

From the ‡Department of Structural Biology, Graduate School of Pharmaceutical Sciences, Hokkaido University, N-12, W-6, Kita-ku, Sapporo, 060-0812, Japan, §CREST, Japan Science and Technology Corporation, Motomachi 4-1-8, Kawaguchi 332-0012, Japan, and ¶Department of Molecular Biology, Graduate School of Pharmaceutical Sciences, Hokkaido University, N-12, W-6, Kita-ku, Sapporo, 060-0812, Japan

DJ-1 is a multifunctional protein that plays essential roles in tissues with higher order biological functions such as the testis and brain. DJ-1 is related to male fertility, and its level in sperm decreases in response to exposure to sperm toxicants. DJ-1 has also been identified as a hydroperoxide-responsive protein. Recently, a mutation of DJ-1 was found to be responsible for familial Parkinson's disease. Here, we present the crystal structure of DJ-1 refined to 1.95-Å resolution. DJ-1 forms a dimer in the crystal, and the monomer takes a flavodoxin-like Rossmann-fold. DJ-1 is structurally most similar to the monomer subunit of protease I, the intracellular cysteine protease from *Pyrococcus horikoshii*, and belongs to the Class I glutamine amidotransferase-like superfamily. However, DJ-1 contains an additional α-helix at the C-terminal region, which blocks the putative catalytic site of DJ-1 and appears to regulate the enzymatic activity. DJ-1 may induce conformational changes to acquire catalytic activity in response to oxidative stress.

DJ-1 was initially identified as a novel oncogene product that transforms mouse NIH3T3 cells in cooperation with activated Ras. DJ-1 is an ~20-kDa protein comprising 189 amino acid residues ubiquitously expressed in various human tissues and with a particularly high level of expression in the testes (1).

SP22[1] or CAP1, a rat homologue of human DJ-1, was subsequently identified as a key protein related to infertility in male rats exposed to sperm toxicants such as ornidazole and epichlorohydrin where DJ-1/CAP1/SP22 levels in the sperm and epididymis decreased with increased rat infertility (2–4). With the exception of DJ-1, no other protein decreased in response to exposure to sperm toxicants, supporting the close relationship between DJ-1 function and male fertility. Recently, Klinefelter *et al.* (5) revealed that DJ-1/CAP1/SP22 was located on the equatorial segment of the matured sperm head and anti-SP22 Ig significantly inhibited the *in vitro* fertilization of hamster oocytes. Thus, DJ-1 may play a role in both zona penetration and membrane fusion steps of fertilization (5, 6).

PIASxα was isolated as a DJ-1-binding protein, which is specifically expressed in the testes and down-regulates the transcriptional activity of the androgen receptor. DJ-1 directly binds to the androgen receptor binding site of PIASxα and absorbs PIASxα from the androgen receptor-PIASxα complex. Thus, DJ-1 is considered to be a positive regulator of androgen receptor-dependent transcriptional activity (7).

Interestingly, a highly conserved amino acid residue Leu-166 in DJ-1 was recently reported to be replaced by Pro in patients with familial Parkinson's disease, PARK7, and thus, this mutation was considered to be responsible for Parkinsonism (8). DJ-1 was also identified as a hydroperoxide-responsive protein, which is converted into a pI variant in response to oxidative stress as with H_2O_2 or paraquat, resulting in the production of reactive oxygen species. Thus, DJ-1 functions as a sensor for oxidative stress (9, 10). Since oxidative stress is closely related to neurodegenerative diseases, there is a great demand for the clarification of the relationship between the DJ-1 mutation and pathogenesis of Parkinson's disease (11).

Although DJ-1 is a small protein of ~20 kDa, it is related to cell transformation, male fertility, oxidative stress response, and Parkinson's disease. However, the molecular mechanism by which DJ-1 exerts these multiple functions remains elusive. Here, we report the first x-ray crystal structure of DJ-1 to get an insight into its functional properties.

MATERIALS AND METHODS

Data Collection—Protein expression, purification, and crystallization will be described elsewhere. All of the diffraction data were collected at 100 K on a RAXIS IV imaging plate detector (Rigaku) using CuKα radiation from a rotating anode x-ray generator. The data collection was performed at a total oscillation range of 142° with a step of 2° for each exposure time of 60 min. The camera distance was 130 mm. The crystal was found to diffract to a resolution of up to 1.95 Å and belong to space group $P3_1$ with unit-cell parameters of $a = b = 75.04$ and $c = 74.88$ Å. The crystal contains two molecules in an asymmetric unit and has a solvent content of 59%. Iridium and mercury derivatives were prepared by soaking the crystals in a reservoir solution containing heavy atom reagents at 293 K. Selenomethionine derivative was expressed in *Escherichia coli* B834(DE3) using an amino acid medium (12) containing selenomethionine instead of methionine. The diffraction data of those derivatives were collected in the same conditions as the native one with the exception that the oscillation range was 180°. All of the data were processed using DENZO and SCALEPACK programs (13). The results of the diffraction data are summarized in Table I.

* This work has been supported by CREST of Japan Science and Technology and by grant-in-aids for Scientific Research on Priority Areas and National Project on Protein Structural and Functional Analyses from the Ministry of Education, Culture, Sports, Science and Technology of Japan. The costs of publication of this article were defrayed in part by the payment of page charges. This article must therefore be hereby marked "*advertisement*" in accordance with 18 U.S.C. Section 1734 solely to indicate this fact.

The atomic coordinates and structure factors (code 1UCF) have been deposited in the Protein Data Bank, Research Collaboratory for Structural Bioinformatics, Rutgers University, New Brunswick, NJ (http://www.rcsb.org/).

‖ To whom correspondence should be addressed. Tel.: 81-11-706-3975; Fax: 81-11-706-4979; E-mail: finagaki@pharm.hokudai.ac.jp.

[1] The abbreviations used are: SP22, sperm protein; CAP1, contraception-associated protein; PIASxα, protein inhibitor of activated STAT; STAT, signal transducers and activators of transcription; GAT, glutamine amidotransferase-like.

TABLE I
X-ray crystallography data statistics

	Data set			
	Native	Se-met	K_2IrCl_6	CH_3HgCl
Data collection statistics				
Resolution (Å)	100-1.90	100-2.5	100-2.5	100-2.5
Concentration (mM)			10	0.1
Wavelength (Å)	1.5418	1.5418	1.5418	1.5418
No. of reflections	145,149	85,565	87,596	87,348
No. of unique reflections	34,488	15,043	15,328	15,348
Completeness (%)	98.2	100	100	100
R_{merge}[a]	0.073	0.054	0.074	0.143
Phasing statistics				
Resolution (Å)		50-2.8	50-4.0	50-2.8
No. of sites		10	6	8
R_{iso}[b]		0.152	0.215	0.212
R_{cullis}[c]				
Working set		0.61	0.69	0.60
Phase set		0.60	0.84	0.59
FOM[d]	0.642			
Refinement statistics				
Resolution (Å)	37.52-1.95			
No. of reflections	32,766			
Completeness (%)	95.3			
R-factor	0.171			
Free *R*-factor	0.194			
No. of protein atoms	2,720			
No. of water molecules	323			
R.m.s.d.[e]				
Bond length (Å)	0.005			
Angles (°)	1.338			

[a] $R_{merge} = \Sigma\Sigma_j|I_j - \langle I\rangle|/\Sigma\langle I\rangle$, where $\langle I_j\rangle$ is the average intensity of reflection j for its symmetry equivalents.
[b] $R_{iso} = \Sigma||F_{ph}| - |F_p||/\Sigma|F_p|$, where F_{ph} and F_p are the derivative and native structure-factor amplitudes, respectively.
[c] $R_{cullis} = \Sigma||F_{ph} \pm F_p| - F_h/\Sigma|F_{ph} \pm F_p|$, where F_h is the calculated heavy atom structure-factor amplitude.
[d] FOM, mean figure of merit.
[e] R.m.s.d., root mean square deviation.

Structure Determination of DJ-1—The initial phasing was performed by multiple isomorphous replacement method using the crystals of the three derivatives. All of the programs used were attached to the CNS program suite (14). After scaling was applied to the data sets of the derivatives, the heavy atom parameters were refined and the multiple isomorphous replacement phases were calculated using the data between resolution of 50 and 2.8 Å. After density modification (15) was applied to the multiple isomorphous replacement map, an initial model consisting of one DJ-1 molecule was placed on the modified electron density map. The other monomer was then generated through non-crystallographic symmetry operations. Initial refinement was performed by the torsion angle molecular dynamic simulated annealing method and bulk-solvent correction against the maximum-likelihood amplitude target. For each cycle, the model was rebuilt manually using the molecular modeling program Turbo-Frodo (16). Throughout the initial refinement, non-crystallographic symmetry constraints were imposed on all of the residues. After the resolution was extended to 2.5 Å, the constraints were lifted and refinement was performed by energy minimization, individual isotropic B factor refinement, and bulk-solvent correction against the maximum-likelihood amplitude target.

RESULTS

Characterization of DJ-1—DJ-1 was cloned into a pGEX6P vector and expressed in *E. coli* BL21(DE3) as a fusion protein with glutathione *S*-transferase. The protein was excised by trypsin and purified by gel exclusion chromatographies. Molecular weight analysis by matrix-assisted laser desorption ionization time-of-flight/mass spectrometry and N-terminal amino acid sequence analysis revealed that the purified protein was intact DJ-1(1–189). The molecular weight in solution was estimated to be 44 kDa by gel exclusion chromatography, suggesting that DJ-1 exists as a dimer in aqueous solution.

Overall Structure of DJ-1—The crystal structure of DJ-1 was solved by multiple isomorphous replacement. The electron density map after density modification was of sufficient quality to allow tracing of most residues in the structure. The model was subsequently refined to 1.95 Å with R = 17.1% and R_{free} = 19.4%, respectively. All of the data collection and phasing and refinement statistics are summarized in Table I.

The final model contains two DJ-1 molecules in an asymmetric unit that form a face-to-face dimer with a 2-fold axis (Fig. 1) and 323 water molecules. The C-terminal Asp-189 is missing because of structural disorder. The dimer formation in the crystal is consistent with the result of gel exclusion chromatography, supporting the notion that the dimer form in the crystal is not due to crystal packing but is physiologically relevant. The overall structure of the DJ-1 dimer is globular with dimensions of 56.1 × 49.5 × 59.6 Å.

Structure of the DJ-1 Monomer—The DJ-1 monomer takes a flavodoxin-like Rossmann-fold, which contains a parallel β-sheet arranged in the order of β2-β1-β4-β5-β7 as a core (17). The β-sheet is flanked by α-helices so that DJ-1 has a three-layered structure (Fig. 2*a*). In addition, there are several secondary structural elements associated with the core, β3, α3, α6, α7, β6, and α9. In particular, β6 forms an anti-parallel β-sheet with β7. The DJ-1 monomer contains seven β-strands and nine α-helices in total (Fig. 2, *a* and *b*). Structure-based sequence alignment was made using human, mouse, *Xenopus*, nematoda, and *Drosophila* DJ-1 and CAP1/SP22, a rat homologue of DJ-1. Most of the conserved residues are involved in the structural core.

Dimer Interface of DJ-1—The dimer interface and the opposite surface of DJ-1 are shown in an electrostatic surface potential presentation (Fig. 3, *a* and *b*). The total area of the buried surface is ~2,600 Å^2. The dimer interface comprises β3, α1, α8, and α9 (Fig. 1). It should be noted that the intermolecular β-sheet is formed among the Val-51, Ile-52, and Cys-53

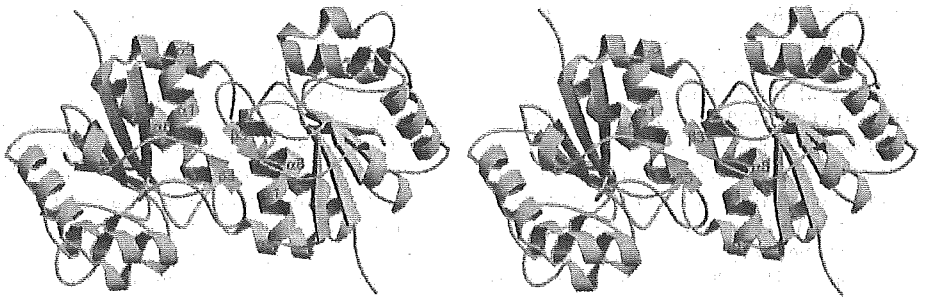

FIG. 1. **The overall structure of the DJ-1 dimer.** A stereo pair of a ribbon diagram of the DJ-1 dimer. The *ribbons* are *colored blue* for monomer A and *green* for monomer B. The four structure elements responsible for the dimer interface are *labeled* in *red*. β3 is formed by dimerization. This figure and Figs. 2*a* and 4 were prepared using MolScript (27) and Raster3D (28).

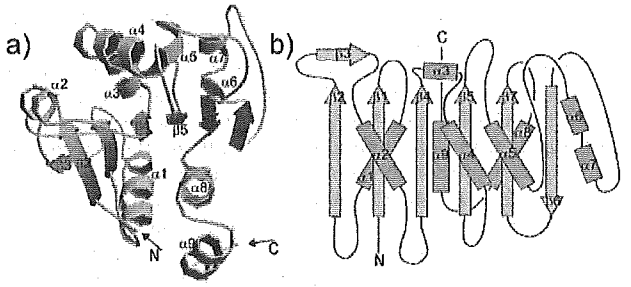

FIG. 2. **The structure of the DJ-1 monomer.** *a*, a ribbon diagram of the DJ-1 monomer. The secondary structure elements are shown in *blue* for α-helices and in *green* for β-strands and are labeled in the figure. Positions of the N and C termini are indicated with *arrows*. *b*, topology diagrams of DJ-1 (*color-coded* as in *a*). The α-helices are represented by *rectangles*, and β-strands are represented by *arrows*.

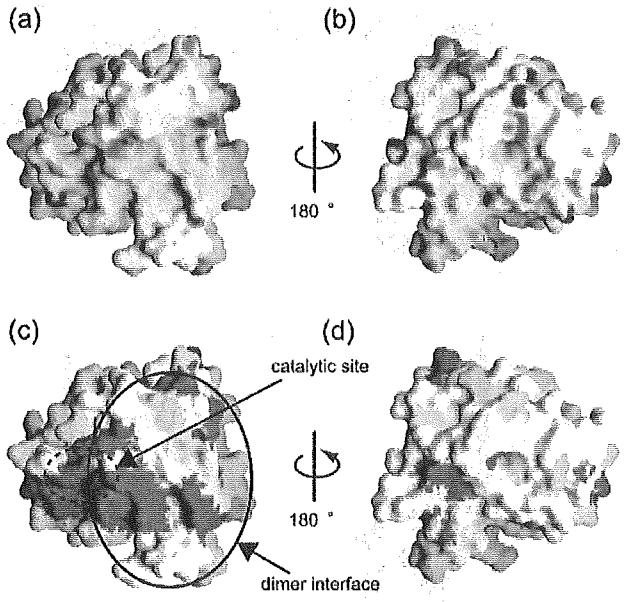

FIG. 3. **Surface representations of the dimer interface and the opposite surface of DJ-1.** The electrostatic surface potential of DJ-1 for the dimer interface (*a*) and the opposite surface (*b*) is shown. *Red* and *blue* represent negative and positive potentials, respectively. The surface model for the dimer interface (*c*) and the opposite surface of DJ-1 (*d*) in which the binding surface is *encircled* with a *solid line* are shown. The conserved and type conserved residues are shown in *red* and *yellow*, respectively. Compared with the opposite surface, the residues on the dimer interface are either conserved or type-conserved. Notably, the residues forming the putative catalytic site (*encircled* with a *dotted line*) are located close to the dimer interface and are highly conserved. Fig. 3 was prepared using GRASP (29).

located on each β3 strand. The distance between the sulfur atoms of Cys-53 is 3.1 Å, slightly far apart to form a disulfide bridge. The interaction between α-helices is mainly hydrophobic but there are several hydrogen bonds and ionic interactions. A number of hydrophobic interactions including the following residues, Met-17, Val-20, Ile-21, Val-23, Val-50, Ile-52, His-126, Phe-162, Pro-184, Leu-185, and Val-186, were observed where half of them (Met-17, Ile-21, His-126, Pro-127, Pro-158, and Phe-162) were completely conserved in human, mouse, rat, *Xenopus*, *Drosophila*, and nematoda DJ-1. In particular, Met-17 and Phe-162 are the core of the hydrophobic interactions and are essential for dimer formation. The conserved (*red*) and type-conserved (*yellow*) residues are mapped on the surface of DJ-1. Notably, the dimer interface consists of the conserved and the type-conserved residues (Fig. 3*c*, *encircled* with a *solid line*) in contrast to the opposite surface (Fig. 3*d*), suggesting that the dimer formation of DJ-1 is correlated with its biological functions.

Structural Similarity of DJ-1 to Other Proteins—Comparison of the DJ-1 structure with the Protein Data Bank (18) data base using the DALI search engine (19) revealed that DJ-1 is structurally most similar to the monomer unit of protease I, an intracellular cysteine protease from *Pyrococcus horikoshii* with a *Z* score of 26.3 and a root mean square deviation of 1.6 Å for 166 residues (Fig. 4, *a* and *b*) (20). The DALI search also revealed that DJ-1 has similar topology to three proteins: the domain of catalase HPII from *E. coli* (17, 21); the subunit of anthranilate synthase TrpG from *Sulfolobus solfataricus* (22, 23); and the domain of GMP synthetase from *E. coli* (Table II) (24). All of the three proteins have flavodoxin-like Rossmann-folds and belong to the Class I glutamine amidotransferase-like superfamily (GAT superfamily) involving thiJ domains (17). With the exception of the domain of catalase HPII where the catalytic cysteine residue is replaced by glycine, all of the proteins belonging to the GAT superfamily have hydrolase activity and contain Cys-His or Cys-His-Asp/Glu as a catalytic group (17, 20–24). The catalytic cysteine residue is structurally well conserved in the GAT superfamily and is located on the short kinked loop connecting an α-helix and a β-strand characterized as the "nucleophile elbow" in α/β-hydrolases (25). As a result, the catalytic cysteine residue falls in an unfavorably allowed region in the Ramachandran plot (25). Actually, in DJ-1, the connecting loop between β5 and α5 was found to form the nucleophile elbow similar to protease I (Fig. 4, *c* and *d*). Cys-106 is located on the loop and has an unfavorable main chain conformation. His-126 is the putative catalytic residue located in close proximity to Cys-106. The residues around the putative catalytic site in DJ-1 are also well conserved in DJ-1 homologues (Fig. 3*c*, residues *encircled* with a *dotted line*). However, there are no acidic residues around His-126 in DJ-1 monomer, whereas in protease I, the neighboring molecule provides Glu-74 to form the catalytic triad (Fig. 4*d*). Thus, we

searched for the possibility to form the catalytic triad in the DJ-1 dimer but did not find any acidic residues. Structural comparison between DJ-1 and protease I revealed that DJ-1 contains an additional α9 at the C terminus, which distinguishes DJ-1 from the rest of the GAT superfamily proteins. α9 and the C-terminal region appear to block the catalytic site of the DJ-1 counterpart and are endowed with regulatory roles (Fig. 4*c*). His-126 is involved in the dimer formation through hydrogen bond interaction with Pro-184 and the hydrophobic interaction with Val-186 of the counterpart, which imposes an unfavorable orientation on the His-126 imidazole ring to form the catalytic dyad and inhibits substrate binding (Fig. 4*c*). Furthermore, α9 may prevent the possible formation of the catalytic triad with an acidic residue on the counterpart as in protease I (Fig. 4*d*). We propose that in the crystal form, DJ-1 does not have any catalytic activity due to blockage by α9 and the C-terminal region but may have a catalytic function after conformational change induced by specific signals or protease digestion. Although we tested the protease activity of DJ-1 using synthetic substrates, we observed only negligible protease activity in its intact form (data not shown). DJ-1 is localized on the equatorial segment of the sperm head where the sperm fuses with oocytes as the sperm matures. In addition, anti-SP22 Ig significantly inhibited *in vitro* fertilization of hamster oocytes (5). Taken together, these results led us to speculate that DJ-1 plays an essential role in zona penetration and in promoting the fusion steps of fertilization where the protease activity of DJ-1 may be tightly regulated.

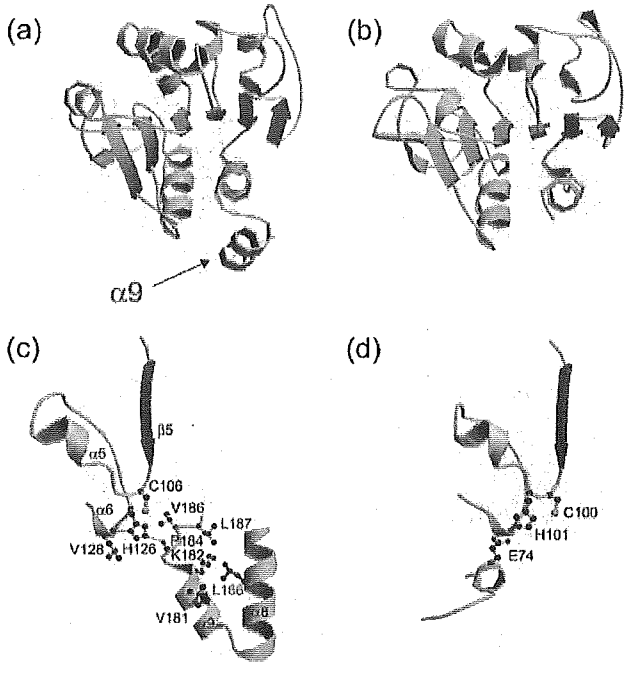

FIG. 4. **Comparison of the monomer structures and the putative catalytic sites between DJ-1 and protease I.** Ribbon diagrams of the monomer subunits of DJ-1 (*a*) and protease I (*b*). Secondary structure is *color-coded* as in Fig. 2*a*. *c*, the region around the putative active site of DJ-1 including β5, α5, and the nucleophile elbow in monomer A (in *blue*) and α8 and α9 in monomer B (in *green*). The residues Cys-106, His-126, and Val-128 in monomer A and Leu-166, Val-181, Lys-182, Pro-184 (a backbone oxygen), Val-186, and Leu-187 in monomer B are shown as *ball-and-stick models*. The His-126 imidazole ring forms hydrogen bonds with the main-chain carbonyl group of Pro-184 (monomer B) and the main-chain amide group of Val-128 (monomer A) are shown by the *dotted lines*. Thus, the His-126 imidazole ring does not take a preferable orientation for protease activity. Leu-166, mutated to proline in PARK7 patients, is shown in *red*. *d*, the region around the active site of protease I including the nucleophile elbow in which the catalytic residue Cys-100 is located. Protease I forms a hexamer, and the catalytic triad is formed in the dimer interface (monomer A is in *blue*, and monomer B is in *green*).

Structural Implication for Parkinson's Disease—A DJ-1 mutation at Leu-166 to Pro was recently found to be associated with PARK7, a monogenic form of human Parkinsonism. Leu-166 is located at the middle of α8, and the mutation appears to break the α-helix. Leu-166 forms a hydrophobic interaction with Val-181, Lys-182, and Leu-187 on α9 and the C-terminal tail (Fig. 4*c*) so that the proline mutation would disrupt the hydrophobic interaction between α8 and α9, destabilizing the dimer interface of DJ-1. Notably, DJ-1 expression is induced by oxidative stress as with H_2O_2 or paraquat and is regarded as an oxidative stress-responsive protein (9, 10). Because reactive oxygen species produced in normal dopamine metabolism have been implicated in neuronal death, oxidative stress in the brain is closely related to the pathogenesis of Parkinson's disease (11). In this context, it is reasonable to assume that DJ-1 functions as an antioxidant protein and any defects may be the cause of Parkinson's disease.

DISCUSSION

DJ-1 is a multifunctional protein and plays essential roles in tissues with higher order biological functions such as the testes and brain. Anti-DJ-1 Ig inhibited the fusion of sperm with an oocyte. Moreover, DJ-1 levels in sperm decreased upon exposure to sperm toxicants and is thought to be responsible for male fertilization. Considering the structural similarity between DJ-1 and the GAT superfamily proteins, we speculate that DJ-1 has protease activity that is inactive in the dimer structure but becomes active by conformation change or protease digestion at the C-terminal region.

DJ-1 was also identified as an oxidative stress responsive protein and was found to be associated with Parkinsonism, a neurodegenerative disease, supporting the notion that DJ-1 is responsible for the quality control of proteins under oxidative stress. Upon oxidative stress, pI of DJ-1 was reported to change from 6.2 to 5.8, suggesting that DJ-1 might adsorb the reactive oxygen species and is modified to acquire a slightly lower pI. Oxidative conversion of sulfhydryl group(s) at a cysteine residue(s) to a cysteine sulfinic acid (Cys-SO_2H) is the most plausible candidate responsible for the pI shifts of hydroperoxide-responsive proteins (9). Mutation of Cys-53 to Ala actually

TABLE II
Structural homologues to DJ-1[a]

Protein	Cα[b]	Z-score	R.m.s.d.[c]	Identity[d]	PDB code
			Å	%	
Protease I	166	26.3	1.6	22	1g2i-A
Catalase HPII	136	16.5	2.0	11	1cf9-A
Anthranilate synthase (TrpG-subunit)	122	7.9	3.2	12	1qdl-B
GMP synthetase	122	7.2	3.1	10	1gpm-A

[a] The structures were compared to that of DJ-1 using the DALI program.
[b] Number of C atoms superimposed between the two structures.
[c] R.m.s.d., root mean square deviation of superimposed C atoms.
[d] The sequence identity is given between the number of Cα toms superimposed.

abolished the formation of the pI variant, confirming that Cys-53 is responsible for oxidative stimuli.[2] Since Cys-53 is located on β3 of the dimer interface, the conversion of Cys to Cys-SO_2H in β3 may destabilize the dimer interface and the DJ-1-specific C-terminal region may be displaced, thus removing the inhibition of protease activity. Proline mutation may abolish the conformation change required for protease activity.

The crystal structure of a heat shock protein, *E. coli* Hsp31, was recently reported (26). Interestingly, its structure is quite similar to that of DJ-1, although an additional domain donates the acidic residues, resulting in the formation of the catalytic triad. However, the catalytic site is completely covered by the inserted domain, which develops a fused hydrophobic surface on the Hsp31 dimer. Thus, Hsp31 appears to sense and digest misfolded proteins, whereas DJ-1 appears to sense oxidative stress and gains the protease activity to digest oxidative damaged proteins.

Although further studies are required to elucidate the relationship of DJ-1 with male fertility, oxidative stress, and Parkinson's disease, the crystal structure of DJ-1 has shed light on the structure-function relationship of DJ-1.

REFERENCES

1. Nagakubo, D., Taira, T., Kitaura, H., Ikeda, M., Tamai, K., Iguchi-Ariga, S. M. M., and Ariga, H. (1997) *Biochem. Biophys. Res. Commun.* **231,** 509–513
2. Klinefelter, G. R., Laskey, J. W., Ferrell, J., Suarez, J. D., and Riberts, N. L. (1997) *J. Androl.* **18,** 139–150
3. Wagenfeld, A., Gromoll, J., and Cooper, T. G. (1998) *Biochem. Biophys. Res. Commun.* **251,** 545–549
4. Welch, J. E., Barbee, R. R., Roberts, N. L., Suarez, J. D., and Klinefelter, G. R. (1998) *J. Androl.* **19,** 385–393
5. Klinefelter, G. R., Welch, J. E., Perreault, S. D., Moore, H. D., Zucker, R. M., Suarez, J. D., Roberts, N. L., Bobseine, K., and Jeffay, S. (2002) *J. Androl.* **23,** 48–63
6. Okada, M., Matsumoto, K., Niki, T., Taira, T., Iguchi-Ariga, S. M. M., and Ariga, H. (2002) *Biol. Pharm. Bull.* **25,** 853–856

[2] T. Taira, manuscript in preparation.

7. Takahashi, K., Taira, T., Niki, T., Seino, C., Iguchi-Ariga, S. M. M., and Ariga, H. (2001) *J. Biol. Chem.* **276,** 37556–37563
8. Bonifati, V., Rizzu, P., van Baren, M. J., Schaap, O., Breedveld, G. J., Krieger, E., Dekker, M. C., Squitieri, F., Ibanez, P., Joosse, M., van Dongen, J. W., Vanacore, N., van Swieten, J. C., Brice, A., Meco, G., van Duijn, C. M., Oostra, B. A., and Heutink, P. (2003) *Science* **299,** 256–259
9. Mitsumoto, A., Nakagawa, Y., Takeuchi, A., Okawa, K., Iwamatsu, A., and Takanezawa, Y. (2001) *Free Radical Res.* **35,** 301–310
10. Mitsumoto, A., and Nakagawa, Y. (2001) *Free Radical Res.* **35,** 885–893
11. Giasson, B. I., Ischiropoulos, H., Lee, V. M., and Trojanowski, J. Q. (2002) *Free Radical Biol. Med.* **32,** 1264–1275
12. LeMaster, D. M., and Richards, F. M. (1985) *Biochemistry* **24,** 7263–7268
13. Otwinowski, Z., and Minor, W. (1997) *Methods Enzymol.* **276,** 307–326
14. Brünger, A. T., Adams, P. D., Clore, G. M., DeLano, W. L., Gros, P., Grosse-Kunstleve, R. W., Jiang, J. S., Kuszewski, J., Nilges, M., Pannu, N. S., Read, R. J., Rice, L. M., Simonson, T., and Warren, G. L. (1998) *Acta Crystallogr. Sect. D. Biol. Crystallogr.* **54,** 905–921
15. Abrahams, J. P., and Leslie, A. G. W. (1996) *Acta Crystallogr. Sect. D. Biol. Crystallogr.* **52,** 30–42
16. Cambillau, C., and Roussel, A. (1997) *Turbo-Frodo*, version OpenGL 1, Université Aix-Marseille II, Marseille, France
17. Horvath, M. M., and Grishin, N. V. (2001) *Proteins* **42,** 230–236
18. Bernstein, F. C., Koetzle, T. F., Williams, G. J., Meyer, E. E., Jr., Brice, M. D., Rodgers, J. R., Kennard, O., Shimanouchi, T., and Tasumi, M. (1977) *J. Mol. Biol.* **112,** 535–542
19. Holm, L., and Sander, C. (1996) *Science* **273,** 595–602
20. Du, X., Choi, I. G., Kim, R., Wang, W., Jancarik, J., Yokota, H., and Kim, S. H. (2000) *Proc. Natl. Acad. Sci. U. S. A.* **97,** 14079–14084
21. Bravo, J., Mate, M. J., Schneider, T., Switala, J., Wilson, K., Loewen, P. C., and Fita, I. (1999) *Proteins* **34,** 155–166
22. Knochel, T., Ivens, A., Hester, G., Gonzalez, A., Bauerle, R., Wilmanns, M., Kirschner, K., and Jansonius, J. N. (1999) *Proc. Natl. Acad. Sci. U. S. A.* **96,** 9479–9484
23. Spraggon, G., Kim, C., Nguyen-Huu, X., Yee, M. C., Yanofsky, C., and Mills, S. E. (2001) *Proc. Natl. Acad. Sci. U. S. A.* **98,** 6021–6026
24. Tesmer, J. J., Klem, T. J., Deras, M. L., Davisson, V. J., and Smith, J. L. (1996) *Nat. Struct. Biol.* **3,** 74–86
25. Ollis, D. L., Cheah, E., Cygler, M., Dijkstra, B., Frolow, F., Franken, S. M., Harel, M., Remington, S. J., Silman, I., and Schrag, J. (1992) *Protein Eng.* **5,** 197–211
26. Quigley, P. M., Korotkov, K., Baneyx, F., and Hol, W. G. (2003) *Proc. Natl. Acad. Sci. U. S. A.* **100,** 3137–3142
27. Kraulis, P. J. (1991) *J. Appl. Crystallogr.* **24,** 946–950
28. Merrit, E. A., and Murphy, M. E. P. (1994) *Acta Crystallogr. Sect. D Biol. Crystallogr.* **50,** 869–873
29. Nicholls, A., Sharp, K., and Honig, B. (1991) *Proteins Struct. Funct. Genet.* **11,** 281–296